C. P. No. 715

C. P. No. 715

MINISTRY OF AVIATION

AERONAUTICAL RESEARCH COUNCIL

CURRENT PAPERS

A Comparison of the Measured and Predicted Flutter Characteristics of a Wing-Aileron-Tab Model

By

H. Hall

LONDON HER MAJESTY'S STATIONERY OFFICE

1965

PRICE 12s 0d NET

U.D.C. No. 533.6.013.422 : 533.693 : 533.694.512 : 533.694.58

C.P. No. 715

August, 1963

A COMPARISON OF THE MEASURED AND PREDICTED FLUTTER CHARACTERISTICS OF A WING-AILERON-TAB MODEL

by

H. Hall

SUMMARY

The paper presents results of wind tunnel flutter tests uwing a wing-aileron-tab model on which it was possible to represent any of the following tab systems; spring, geared, trim or servo. Prediction of the flutter characteristics has been made in the trim tab case using three sets of aerodynamic derivatives and fair agreement has been reached with the measured characteristics. A comparison has also been made of the measured characteristics with those predicted by the latest flutter criteria and possible modifications to the basic flutter frequency assumption used in deriving the criteria are discussed. One modification suggested is such that the basic flutter frequency is virtually dependent on the frequency in a single degree of freedom. The criterion form that results from such a single frequency approximation is investigated.

Replaces R.A.E. Tech. Note No. Structures 338 - A.R.C. 25 229

CONTENTS

TABLES

TABLES (Continued)

ILLUSTRATIONS

ILLUSTRATIONS (Continued)

ILLUSTRATIONS (Continued)

1 INTRODUCTION

A number of flutter incidents over the past decade have involved flutter of a control surface-tab combination. The work reported in this note on a model wing fitted with aileron and tab is complementary to earlier general theoretical investigations[1,2,3,4] on the flutter of tab systems.

The model was virtually rigid and had freedom in roll at its root. It carried an aileron and tab whose circuit stiffness characteristics could be varied by suitable torsion springs. Helical springs governing the oscillatory rolling motion of the model could also be varied. Provision was made for mass-balancing both control surfaces and for variation of the gearing between tab and aileron motion.

The model provided a system whose inertia and elastic properties were known accurately and in which elastic properties could be readily varied. Controlled structural information was thus available for inclusion in a flutter calculation and the magnitudes assigned to the oscillatory aerodynamic forces were consequently the most doubtful features of the calculation.

Two basic ways of determining the aerodynamic forces were employed. One way was to use the available experimental data for oscillatory derivatives. Two different sources of this information were available. One source concerned a wing of the same aspect ratio fitted with a full-span aileron only. The other source concerned a two-dimensional wing having a full-span aileron and tab. The controls in these two sources did not have the same chord ratios as the model considered here, and somewhat arbitrary factors were applied to these derivatives in order to obtain a set appropriate to this model.

The other way of determining the aerodynamic forces was an empirical method of estimating the oscillatory derivatives, suggested by Guyett[5] during the course of the flutter calculations. It involves the use of steady motion derivatives, and these were determined in two ways - by measurement and by estimation. The methods employed to measure the steady motion derivatives were as follows. Normally the moment needed to balance the applied aerodynamic moment for a set control angle at a particular wind speed was measured. However, for the control derivative due to rotation of the same control, the derivative was determined additionally from a knowledge of the wind speed at which the control was blown back through a predetermined angle against the action of a spring inserted in the control hinge. For the estimation of the steady motion derivatives for use in the Guyett method well established techniques were employed.

The experimental results also provide a basis for comparison with the latest approximate formulae for flutter prediction due to Molyneux[6]. The comparison has been made using two of the sets of aerodynamic derivatives mentioned above. As a result some comments are made on the efficacy of the formulae in determining the binary flutter boundaries. Molyneux suggests that modifications may be required to the basic frequency approximation on which the criteria depend for particular binary systems and this suggestion has been investigated. The form of criterion that results from a somewhat different flutter frequency approximation to that adopted by Molyneux has been derived and applied to this system.

This introduction outlines the scope of the work reported on in the note. Sections 2 and 3 are intended primarily for the specialist reader and describe in some detail the work done and the results obtained. The conclusions from the work are given in Section 4 and non-specialist readers may prefer to pass to this section immediately.

2 EXPERIMENTAL INVESTIGATIONS

2.1 Description of rig and model

The rig and model are sketched in Fig.1 and the main dimensions of the wing are given in Table 1. The model half wing was mounted vertically above a reflector plate (not shown in Fig.1) and was free to roll about its root end. An approximately half span aileron and one third span tab were mounted outboard. The wing was solid, made from spruce with a main spar of steel channel. Five plywood ribs hung on a dural tube formed the framework for the aileron which had a hollow plywood nose. A solid cedar block pinned and glued to the furthest outboard ribs formed the trailing edge of the section of the control not containing the tab. The aileron surface was of fabric which was doped to give drum tightness. The tab consisted of a dural tube, forming the nose section, to which was glued and screwed a shaped balsa block to form the trailing edge. Both aileron and tab were free to rotate on ball races and friction damping was small.

The wing main spar had an extension member below the roll axis and helical springs from this member to the mounting frame provided stiffness in roll. The most general tab system that could be represented on the model had the spring connections K_A, K_B, K_C shown in Fig.2. By including suitable combinations of these springs the following systems could be simulated. Thus, when

(1) K_A and K_C were included. A geared tab system was represented. Spring K_A represented the stiffness of the control circuit operating the control surface. K_A is normally large compared with K_C.

(2) K_A and K_B were included. A trimming tab system was represented. K_A again represented the stiffness of the control circuit operating the control surface. K_A is normally large compared with K_B.

(3) K_C only was included. A pure aerodynamic servo tab system was represented when the follow up ratio was positive.

(4) K_A, K_B, K_C were included. A spring tab was represented. The spring-tab system can be represented in several ways, perhaps the most general arrangement being that shown in Ref.3. There was no direct equality between any one spring of this system and those of the general spring tab system, but the combined effect of the springs was to provide an elastic matrix which could be directly related to that for any spring tab system.

The follow up ratio is defined as the ratio tab angle/aileron angle when the aileron is rotated with the tab control lever held fixed by an infinitely stiff spring K_C. For a trim tab, however, it is physically possible to move the control without producing any relative motion of the tab and in this sense the follow up ratio is effectively zero.

Provision was made for mass-balancing both the aileron and tab. Aileron mass-balance was effected by adding weights on an arm forward of the hinge line. The mass-balance weight oscillated in a cut out in the wing and was shaped so that its intrusion into the airstream affected the flow as little as possible. Tab mass-balance was in the form of dural, steel or lead quadrants bolted to a wheel whose centre was concentric with that of the tab tube and which was bolted to it.

The tab wheel was connected to a lever which had independent freedom in rotation about the aileron hinge line (Fig.3). Incorporated in the lever were two attachment points, one each side of the aileron. The connection between aileron and tab was by means of a wire joining the attachment points and passing around the wheel rim. The wheel was built up of several discs of varying radii and by passing the wire around the rims of these, several gear ratios between aileron and tab were obtained.

2.2 Wind tunnel measurements

2.2.1 Flutter tests

Tests were made over a wide range of the available variables. Rolling frequency was varied between 1.1 and 5.6 c.p.s., uncoupled aileron frequency between 0 and 18 c.p.s. and uncoupled tab natural frequency between 0 and 16.6 c.p.s. In the tests the steel tab mass-balance weights were situated in their furthest aft position. No mass-balance was fitted to the aileron. The follow up ratios adopted for the tests were N = ±3 and for the trim tab case N = 0. Flutter speed was measured in all the tests and some readings of flutter frequency were taken.

2.2.1.1 Flutter test results

The results of the flutter tests are shown in Figs.4-17. Figs.4-8 show the results of the tests in which there was no gearing between the tab and aileron motion (trim tab). The effect of reduction in uncoupled aileron frequency is shown progressively moving from Fig.4 to Fig.8. Each figure shows graphs of critical flutter speed plotted against uncoupled tab frequency for several values of uncoupled rolling frequency. A particular feature of the tests was the ease with which particular types of flutter could be subdued to enable other flutter branches to be followed into doubly unstable regions. This assisted in subsequent interpretation of the results, and is illustrated in the figures by overlapping flutter boundaries. In discussing the results attention is concentrated on the lower flutter speed boundary.

Fig.4 shows that two types of flutter were found at this value of aileron natural frequency (16.2 c.p.s.). Aileron rotation-tab rotation type flutter occurred for all values of rolling frequency and the critical speeds were

independent of rolling frequency. The minimum flutter speeds for this type of flutter were associated with a tab frequency of approximately 12 c.p.s. The second type of flutter found, occurring at much lower speeds, was wing roll-tab rotation and this existed for tab frequencies below the rolling frequency except for the lowest rolling frequency case tested. It seems likely that the small amount of damping in the tab bearings was sufficient to suppress the flutter in the latter case.

The reduction in aileron frequency to 8.8 c.p.s., Fig.5, had little effect on the overall picture but two points of difference occurred. Lower flutter speeds were obtained for the aileron rotation-tab rotation type flutter and the minimum flutter speed occurred at a tab frequency of approximately 7.5 c.p.s.

There were further points of difference in the results for tests with aileron frequency reduced to 5.9 c.p.s., Fig.6. The wing roll-tab rotation type flutter had now been replaced by a ternary wing roll-aileron rotation-tab rotation flutter. The limits of this ternary type were, however, much the same as the binary type it had replaced. The minimum speed of the aileron-tab type flutter generally now occurred at a tab frequency of approximately 2.5-3.0 c.p.s.

The results for the tests with an aileron frequency of 3.6 c.p.s., Fig.7, were more complicated. With roll frequencies of 1.1 c.p.s. and 2.3 c.p.s., only aileron rotation-tab rotation type flutter was obtained, the flutter speed increasing with increasing tab frequency. At a roll frequency of 3.5 c.p.s. the flutter at low tab frequencies was initially of the ternary wing roll-aileron rotation-tab rotation type, changing to aileron rotation-tab rotation flutter as the tab frequency increased; at a tab frequency of about 10 c.p.s. a wing roll-aileron rotation flutter branch was obtained at a speed considerably lower than the aileron rotation-tab rotation type. For higher roll frequencies the flutter was of the aileron rotation-tab rotation type at low tab frequencies, changing to the wing roll-aileron rotation-tab rotation type and then to the wing roll-aileron rotation type as the tab frequency increased.

The results for a free aileron are shown in Fig.8. For all rolling frequencies the patterns obtained for aileron-tab flutter were similar. In the lower rolling frequency cases the flutter was initially of the ternary type changing to wing-aileron as the tab frequency increased, but without any significant change of flutter speed. For the higher rolling frequencies (4.8 and 5.6 c.p.s.) this pattern was modified by a limited region of aileron-tab flutter that occurred for tab frequencies near zero.

It should be noted that the distinction between two types of flutter which merged into one another was largely a visual one. Thus, the apparent change from wing-aileron-tab flutter to wing-aileron flutter noted above may have been due to the amplitude of tab vibration in the ternary flutter becoming extremely small for the higher values of tab circuit stiffness.

The results of the tests in which the follow up ratio between aileron and tab was +3 are shown in Figs.9-13 (servo and geared tabs). These results are not directly comparable with the zero follow up ratio case as the wing to tab connecting spring makes a contribution to the aileron stiffness. Table 2 gives the aileron and tab natural frequencies corresponding to various combinations

of the connecting springs. Thus, for the no aileron spring case, the aileron natural frequency varies between zero for the free tab and 7 c.p.s. for the wing to tab spring 7T.

Results for the no aileron spring case are shown in Fig.9. At the lowest rolling frequency the flutter was mainly binary aileron rotation-tab rotation but at lower tab frequencies both binary wing roll-aileron rotation and ternary flutter were found at extremely low speeds. For the next higher rolling frequency the flutter was of the ternary type, again at very low speeds. At the higher rolling frequencies the flutter was mainly ternary type but at low tab frequencies binary aileron rotation-tab rotation flutter was found.

The results for the tests in which the wing to aileron connecting spring 1A was used are shown in Fig.10. For low values of rolling frequency flutter was usually aileron rotation-tab rotation type, the critical speed increasing with tab frequency. At higher rolling frequencies the flutter was generally of the ternary type but at the highest rolling frequency a region of aileron rotation-tab rotation flutter was obtained at low tab frequencies.

The results for tests in which the aileron to wing connecting spring 2A was used are shown in Fig.11. Binary aileron-tab flutter was obtained for all combinations of wing rolling and tab natural frequencies.

A further increase in the stiffness of the aileron connecting spring produced results which are shown in Fig.12. Binary aileron-tab flutter occurred for all values of rolling frequency, but at the higher values of rolling frequency and the lower tab frequencies, a region of binary wing roll-tab rotation flutter was also found. The extent of this flutter region was governed by the rolling frequency.

Test results for the highest stiffness aileron connecting spring are shown in Fig.13, they are similar to the preceding set in respect of the flutter types obtained. Flutter of the wing-tab type was obtained at a lower rolling frequency than in the previous case and there was no overlapping of the flutter bands.

The results of the tests for which the follow up ratio N between aileron and tab was -3 are shown in Figs.14 to 17.

No results are plotted for the no aileron spring case as in all the tests apart from the no tab spring case, divergence of the aileron-tab system occurred which was limited by the stops on aileron movement. At this aileron position a vibration of the tab took place which was probably due to the stalled flow.

The results of tests with aileron connecting spring 1A fitted are shown in Fig.14. A region of aileron-tab flutter was obtained for all roll frequencies, a region of ternary flutter was obtained for tab frequencies near zero for roll frequencies of 2.3 c.p.s. and 3.5 c.p.s. and a further region of ternary flutter was obtained at higher tab frequencies for the three highest roll frequencies. With tab frequencies above about 10 c.p.s. aileron-tab divergence occurred at a speed of about 50 ft/sec and the stalled type flutter was then found.

The results of tests with the next stiffest aileron spring (2A) fitted are shown in Fig.15. At low rolling frequencies, only aileron-tab flutter was found but as this frequency was increased the ternary type flutter appeared at high and low tab frequencies. The aileron-tab type remained at intermediate tab frequencies.

Test results for the aileron connecting spring 3A fitted are shown in Fig.16. The results are broadly similar to those for spring 2A (Fig.15) except that the branch of ternary flutter at high tab frequencies is eliminated and that at lower tab frequencies changes to binary wing-tab flutter.

Similar remarks apply to the results for tests with the highest stiffness aileron spring shown in Fig.17.

We may summarise the test results as emphasizing the complexity of the flutter problem for a three degree of freedom system of this type. Large changes may be produced in the flutter characteristics by changes in the follow up ratio between aileron and tab, by variation of the circuit stiffnesses of aileron and tab and of the stiffness in the main surface mode of vibration.

2.2.2 Derivative measurements

In view of the uncertainty over the absolute values of some of the oscillatory aerodynamic derivatives due to aileron and tab rotation, which were to be used in the associated theoretical work, it was decided to obtain these using the method suggested by Guyett[5]. To apply this method it is necessary to know the corresponding steady state derivatives and tests were made to determine these.

The particular oscillatory derivatives in question were ℓ_β, ℓ_γ, h_β, h_γ, t_β, t_γ and the corresponding damping derivatives (see Table 4 for values of these derivatives). The lift derivatives ℓ_β and ℓ_γ were determined from measurements of the restoring moment required to hold the wing in the neutral position against the rolling moment resulting from a set aileron or tab angle. The force which produced this restoring moment was applied at a point 19.75 in. below the wing rolling axis. Tests were made for several control angles and wind speeds and from the results graphs of rolling force against control angle were plotted. The rolling moment due to applied aileron was determined with the tab locked to the aileron and that due to the tab with the aileron locked to the wing.

Similarly, the hinge moment derivative, h_γ was determined from measurements of the moment necessary to hold the aileron in its neutral position against the hinge moment resulting from a set tab angle. Tests were made for several tab angles and wind speeds and from the results graphs of aileron force against tab angle were plotted. In these tests and all hinge moment tests the wing was at zero incidence.

The hinge moment derivatives h_β and t_γ were determined from measurements of the moment needed to balance the aerodynamic hinge moment due to control displacement. The results of the tests were plotted as graphs of applied force

against control angle. Further tests were done in which the tab hinge moment was measured by determining the wind speed at which the tab returned to a datum position slightly displaced from the neutral having been offset in the wind-off condition by a known disturbing force acting against a spring. This last set of tests was done as a check on the results of the first series of tab hinge moment measurements which showed a good deal of scatter.

Attempts were made to measure the tab hinge moment due to control rotation but were not successful. The moment was very small and the results were too inconsistent to provide a satisfactory basis for estimating an oscillatory derivative.

2.2.2.1 Results

The results of the experiments to determine the steady state derivatives are shown in Figs.18 to 23 inclusive.

Tests were made with and without trailing edge wires fitted to the tab. At the commencement of the flutter tests little difference could be detected in the flutter characteristics with and without the wire fitted and in consequence all subsequent tests were made without trailing edge wire. However, the best results for the rolling and hinge moments were obtained with trailing edge wire fitted to the tab. The best results were taken to be those which had least scatter and indicated some degree of non-linearity of the appropriate forces and moments over the control angles near to neutral. The largest amounts of scatter were associated with the small tab disturbing force due to tab angle at the speeds at which the tests were made. In both this case and that of the rolling force due to tab angle, the force for nominally no tab angle was finite. The measurements of the tab hinge moment using wind speed as a variable produced better results in that scatter was reduced and a zero hinge moment for zero tab angle could be interpolated.

A set of derivatives appropriate to the oscillatory case were determined from these results using Guyett's method[5] in which aerodynamic stiffness derivatives depend on the rate of change of the appropriate steady motion rolling and hinge moments with control angle. Table 3 gives the values of the measured steady motion derivatives, expressed in the flutter notation for zero frequency parameter, and compares them with those calculated from the information given in Refs.7 and 8. It can be seen that in all cases but one the predicted values are greater than those measured.

3 THEORETICAL INVESTIGATIONS

3.1 Flutter calculations

Calculations were made initially using two sets of aerodynamic derivatives and these were:-

(i) A set based on a series of derivative measurements by Molyneux[9] and Wight[10] modified for aspect ratio (Method 1) in the manner outlined below (a).

and (ii) A set based largely on steady motion aerodynamic derivatives measured on this wing (Method 2), outlined at (b) below.

(a) The measurements made by Molyneux were for a wing of the same aspect ratio as the one on which these tests were made, but which had a 20% chord full span aileron. Wight's measurements were on an effectively two-dimensional wing having a 20% chord full span aileron and 8% chord full span tab. For the calculation the derivatives ℓ_z, $\ell_{\dot{z}}$, h_z, were taken directly from Molyneux's work. The values assigned to ℓ_β and h_β were obtained from Molyneux's work by taking account of the different values of aileron chord E_β and the fact that the aileron spans were different for this model and his. The factor to take account of the difference in aileron chord was assumed to be the ratio of the two-dimensional theoretical values of the derivative at a particular frequency parameter and the appropriate values of chord ratio while the factor to take account of difference in aileron span was based on the assumption that the derivative was inversely proportional to $\left(1 + \frac{0.8}{A}\right)^2$, where $A = 2 \times \frac{\text{aileron span}}{\text{aileron chord}}$. Values of h_γ, t_β and t_γ were obtained from Wight's measurements by factoring for E_β, the tab chord E_γ and aspect ratio in a similar manner. The remaining stiffness derivatives were obtained from theoretical two-dimensional values at the appropriate frequency parameter modified for aspect ratio.

Damping derivatives were obtained in a similar way to the stiffness derivatives, the aspect ratio factor here depending on $\left(1 + \frac{0.8}{A}\right)$.

(b) Oscillatory derivatives, appropriate to a frequency parameter of zero, were obtained from the steady motion hinge and rolling moments by equating these to the corresponding moments expressed in terms of a flutter derivative. Thus for example,

$$\text{Steady aileron hinge moment per unit tab angle} = \rho V^2 \, sc_m^2 \int_{\text{tab}} (-h_\gamma) d\eta .$$

Having obtained the zero frequency parameter flutter derivative the next step was modification for frequency parameter effects. The modification depends on the derivative. For the derivatives $(-h_\beta)$, $(-h_\gamma)$ and $(-t_\gamma)$ the zero frequency parameter derivative was multiplied by the ratio of the two-dimensional theoretical value of the derivative at the appropriate frequency parameter to that at zero to give the value used in the calculation. The damping derivatives corresponding to these stiffness derivatives were obtained by multiplying by the ratio of the theoretical two-dimensional damping to stiffness derivatives at the appropriate frequency parameter.

The derivatives ℓ_β and ℓ_γ were obtained by a somewhat different procedure. The zero-frequency parameter derivatives were multiplied by the ratio of the equivalent constant strip derivatives[5], for a wing of this aspect ratio, at the appropriate frequency parameter to that at zero. The corresponding damping derivatives were obtained from the stiffness derivatives by multiplying by the

ratio of the equivalent constant strip damping to stiffness derivatives at the appropriate frequency parameter.

The values of ℓ_z and $\ell_{\dot{z}}$ measured by Molyneux were used directly in the calculation. The derivative t_β was given the value obtained from Wight's measurements and the damping derivative likewise. Other derivatives were assigned values as follows - all stiffness derivatives depending on vertical translation z were made zero following a suggestion by Minhinnick[11]. The corresponding damping derivatives, which in both Minhinnick's and Guyett's theories would be put equal to the corresponding stiffness derivative due to pitch of the main surface were in fact put equal to zero. The effect on the flutter coefficients of making this approximation was negligible.

The two sets of derivatives are compared in Table 4 together with a further set in which the aspect ratio correction factors (Method 3) are based on that of the portion of the wing including the appropriate control rather than the control itself (Method 1). It can be seen that the latter set is in better agreement with the derivatives obtained from the steady motion measurements (Method 2).

In both sets of calculations elastic coefficients were put equal to the direct inertia coefficients multiplied by the square of the natural frequency in the appropriate degree of freedom.

It was apparent when the calculations were completed that, in general, the derivatives based on the measured steady motion derivatives yielded the better agreement with measured characteristics but that neither gave very good agreement for flutter speed. Calculated speeds tended to be higher than the experimental values. The fact that Method 2 derivatives are superior to Method 1 is probably due to the fact that they were a more consistent set. The important derivatives were actually measured on this wing whereas with Method 1 the derivatives were obtained from measurements on two different models and somewhat arbitrary factors were applied to these measurements in order to obtain derivatives appropriate to this model.

In order to obtain better agreement for flutter speeds, it seemed likely that a set of derivatives was required that had larger values than either of the sets considered above. One possibility was to use the set based on predicted steady motion derivatives; we have already noted, para.2.2.2.1, that these are in general larger than the corresponding measured values. A second possibility was to use the measured steady values but instead of taking values of hinge moment and rolling moment per unit control angle over the linear portions of the curve as had been done previously to take the slope of the curves corresponding to zero incidence. In view of the fact that moments for small control angles had to be interpolated it was decided that this procedure did not provide a sufficiently firm basis for establishing a set of derivatives in this instance and accordingly the predicted steady motion set was used. It is felt that, in a particular case, if moments corresponding to small control angles can be determined then the slopes over the central region of control angles will provide the best basis for determining an oscillatory set of derivatives.

The results of the flutter calculations on the trim tab system based on Method 2 derivatives and the predicted steady motion derivatives Method 4 are plotted, together with the experimental results, in Figs.24 and 26.

3.2 Comparison of experimental and calculated results

Calculated flutter speeds are plotted for a limited number of wing rolling and aileron natural frequencies, but these are sufficient to show the trends of the results.

Fig.24 shows the results corresponding to an aileron frequency of 8.8 c.p.s. The calculations are in general agreement with the experiment for the flutter characteristics; the reservation that we noted in para.2.2.1.1 concerning identification of flutter types being apposite in this respect. The tab frequencies at which the minima of aileron-tab flutter occur are predicted reasonably accurately by the calculations. Critical speeds for this type of flutter are generally unconservative using Method 2 and conservative using Method 4, this being particularly so for the higher tab frequencies. The limiting tab frequency for the wing-(aileron)-tab flutter band is adequately predicted but the speeds for low tab frequencies are unconservative.

Fig.25 shows the results corresponding to an aileron frequency of 3.6 c.p.s. The calculations predict the types of flutter obtained in practice quite adequately for the cases considered. Both methods predict unconservative speeds particularly for the ternary type flutter at the higher values of tab frequency. Method 4 leads to better agreement with the measured speeds for both values of rolling frequency and predicts the bounds of the flutter types in terms of tab frequency, rather better than Method 2.

Fig.26 shows the results corresponding to a free aileron. The agreement in this case is significantly poorer than for either of the cases where aileron stiffness was present. Both methods predict a band of aileron-tab flutter at low tab frequencies in the highest rolling frequency case which was not found in practice. The predicted speeds of the ternary type flutter to which the aileron-tab type changes are higher than the experimental, Method 4 giving slightly the better agreement of the two. In the intermediate roll frequency case Method 4 leads to the better agreement for flutter speeds, though here again a band of aileron-tab flutter is predicted at low tab frequencies. Calculated results for the lowest roll frequency case show discrepancies from the experimental results. In particular Method 4 predicts two bands of flutter instead of the one continuous band found in the experiment. Flutter speeds for higher tab frequencies are, however, in very good agreement with those measured. Method 2 does predict this continuous branch but it gives unconservative speeds.

To summarise these comparisons. Both methods of calculation yield reasonable approximations to the flutter types obtained in practice particularly for the cases where aileron stiffness is present. The speeds calculated using Method 4 are in rather better agreement with those measured than those obtained using Method 2.

3.3 Comparison of the experimental results with some flutter criteria

Molyneux has suggested specific criteria formulated in terms of basic structural and aerodynamic data, to define the bounds of wing flexure-torsion,

wing flexure-aileron rotation and wing torsion-aileron rotation flutter. The second and third of these have been adapted in the present investigation to yield criteria applicable to wing roll-aileron or tab rotation flutter and aileron rotation-tab rotation type flutter respectively.

The criteria adopted are*

(a) Wing roll-control rotation

$$\left(\frac{d_8\, m_r\, k_c^2}{m_c\, x_c^2} + 1\right) X^2 + 4\left(1 - \frac{d_{10}\, \rho_o\, \ell_c}{E_c\, m_c\, x_c}\left\{\frac{V}{\omega_R}\right\}^2\right) = 0 \qquad (1)$$

where

$$X = \left(\frac{\omega_c}{\omega_R}\right)^2 - 1 - \frac{d_{12}\, \rho_o\, (h.m)_c}{E_c^2\, m_c\, k_c^2}\left\{\frac{V}{\omega_R}\right\}^2 \qquad (2)$$

and where m_r = wing mass/unit length at reference section

$k_c\, c_c$ = radius of gyration of control section at reference axis

c_c = control surface chord at reference axis

m_c = control surface mass/unit length at reference section

$x_c\, c_c$ = distance of centre of gravity of control surface aft of hinge line at reference section

$E_c = c_c/c_r$

c_r = wing chord at reference section

V = flutter speed

ω_R = wing natural frequency in roll

ω_c = control surface natural frequency

ℓ_c = aerodynamic derivative for lift due to control surface rotation

$(h.m)_c$ = aerodynamic hinge moment derivative due to control surface rotation

* It should be noted that these are not the exact forms given by Molyneux. He includes a term in X in the criterion equations (1) and (3) but it has been found in practice that this term usually has little effect on the criterion bounds. In general the coefficient of X is small compared with those of X^2 and the constant term and hence its effect on the solution for X is small. Unless otherwise stated this approximation has been made throughout.

$$d_8 = \frac{\int_w c^2\,d\eta \int_c c^4\,d\eta}{\left(\int_c c^3\,d\eta\right)^2}, \quad d_{10} = \frac{c_r^2 \int_c c\,d\eta}{\int_c c^3\,d\eta}, \quad d_{12} = \frac{c_r^2 \int_c c^2\,d\eta}{\int_c c^4\,d\eta}$$

and the subscripts w and c indicate integration over the wing and control respectively.

(b) Aileron rotation-tab rotation

$$\left(\frac{d_{13} m_A k_A^2 k_t^2}{m_t E_2^2 (dx_t + k_t^2)^2} + 1\right) X^2 + 4\left\{1 - \rho_o\left[\frac{h_\beta}{d_3 m_A E_A^2 k_A^2} - \frac{d_{17} h_\gamma}{m_t E_2^2 (dx_t + k_t^2)}\right]\left(\frac{V}{\omega_A}\right)^2\right\}$$

$$\left\{1 - \rho_o\left[\frac{h_\beta}{d_3 m_A E_A^2 k_A^2} - \frac{d_{17} t_\beta}{m_t E_2^2 (dx_t + k_t^2)}\right]\left(\frac{V}{\omega_A}\right)^2\right\} = 0 \qquad (3)$$

where $$X = \left(\frac{\omega_T}{\omega_A}\right)^2 - 1 + \rho_o\left[\frac{h_\beta}{d_3\ m_A\ E_A^2\ k_A^2} - \frac{d_{12}\ t_\gamma}{m_t\ E_2^2\ k_t^2}\right]\left(\frac{V}{\omega_A}\right)^2 \qquad (4)$$

and where $E_2 = \frac{c_T}{c_A} = \left(\frac{c_T}{c_A}\right)_r$

$E_A = \frac{c_A}{c} = \left(\frac{c_A}{c}\right)_r$

c_T = tab chord

c_A = aileron chord

c = wing chord

dc_T = distance of aileron hinge line forward of tab hinge line

Subscript r denotes lengths at the reference section.

$$d_{13} = \frac{\int_A c_A^4 \, d\eta}{\int_T c_A^4 \, d\eta}, \quad d_3 = \frac{\int_A c^4 \, d\eta}{c_R^2 \int_A c^2 \, d\eta}, \quad d_{12} = d_{17} = \frac{c_{A_r}^2 \int_T c^2 \, d\eta}{\int_T c_A^4 \, d\eta}$$

and the subscripts A and T indicate quantities appropriate to the aileron and tab respectively.

A graph of equations (1) or (3) in which $\left(\frac{V}{\omega_1}\right)^2$ is plotted against X is a parabola and the criterion stipulates that points within this parabola are those at which flutter may occur (ω_1 being the uncoupled natural frequency of the first of the binary modes). The method of applying the criterion is to plot the variation of X with $\left(\frac{V}{\omega_1}\right)^2$ determined from equations (1) or (3) assuming values of $\left(\frac{V}{\omega_1}\right)^2$. The resulting curve represents the flutter boundary. Speeds achieved at points on the flight envelope are used in equations (2) and (4) to determine the corresponding values of X. If the resulting points $\left\{X, \left(\frac{V}{\omega_1}\right)^2\right\}$ lie on or within the criterion parabola then the critical flutter speed will be achieved or exceeded at the corresponding points on the flight envelope.

Molyneux points out in his paper that the ultimate limitation on the application of the criterion is how justifiable is the basic assumption that the flutter frequency is the root mean square of the uncoupled frequencies. He makes the suggestion that closer agreement for particular systems may be obtained by assuming that the flutter frequency is given by

$$\omega^2 = \left\{\frac{1}{1+B}\right\}\left\{\omega_1^2 + \frac{C_{11}}{A_{11}} V^2 + B\left(\omega_2^2 + \frac{C_{22}}{A_{22}} V^2\right)\right\}$$

where B is a frequency weighting factor appropriate to a particular binary system

ω_1, ω_2 are the uncoupled natural frequencies of the modes

A_{11}, A_{22}, C_{11}, C_{22} are the structural inertia and aerodynamic stiffness coefficients of the two modes

V is the flutter speed

Using this frequency approximation the most general form of the criterion equation for wing roll-control rotation flutter for example becomes

$$B\left(\frac{d_8\, m_r\, k_c^2}{m_o\, x_c^2} + B\right) X^2 + (1 + B)\, B\left\{2 - \frac{d_{10}\, \rho_o\, \ell_c}{E_c\, m_c\, x_c}\left(\frac{V}{\omega_R}\right)^2\right\} X$$

$$+ (1 + B)^2 \left\{1 - \frac{d_{10}\, \rho_o\, \ell_c}{E_c\, m_c\, x_c}\left(\frac{V}{\omega_R}\right)^2\right\} = 0$$

where $X = \left(\frac{\omega_c}{\omega_R}\right)^2 - 1 - \frac{d_{12}\, \rho_o\, (h.m)_c}{E_o^2\, m_c\, k_c^2}\left(\frac{V}{\omega_R}\right)^2$.

The basic criterion is the special case of this with B = 1 and with the X term omitted. A further reservation on the use of the criterion is that it may only be expected to produce satisfactory results when the basic aerodynamic derivatives used in it are such that a full scale flutter calculation based upon them will lead to good agreement between calculated and experimental characteristics.

The model inertia characteristics have been used in the application of the criteria and the results are shown in Figs.27 to 30. In order to make both abscissae and ordinates on these graphs non-dimensional, ordinates have been plotted as $\left(\frac{v}{\omega_1}\right)^2$ where $v = \left(\frac{V}{c_r}\right)$. On each figure the derivatives that have been used to obtain the criterion and experimental bounds are indicated.

The result of the application of the criterion to wing roll-aileron rotation flutter (N = 0) is shown in Fig.27 together with the corresponding experimental results for aileron frequencies of zero and 3.6 c.p.s. It can be seen that within the range that Molyneux considers his criterion to be valid i.e. $-0.5 < X < 0.5$, hereafter called the central range of X, the agreement between the experimental curve and the criterion curve is not good, particularly in the negative range of X. An attempt has been made to improve the agreement by applying the frequency weighting factor B = 1/10 and the appropriate curves are shown on the figure (the effect of the term in X in the criterion equation is negligible in this case too). The agreement is now very good in the positive range of X both in absolute value and shape and somewhat improved in the negative range. The frequencies found in practice are compared with those estimated by the frequency approximation, Method 4 derivatives, in Table 5 and it can be seen that the approximation with the frequency weighting factor B = 1/10 is a much better one.

The application of the criterion to wing roll-tab rotation flutter (N = 0) is shown in Fig.28 together with the corresponding test results for two rolling frequencies of 4.8 and 5.6 c.p.s. The Method 4 derivatives are seen to give relatively better agreement between experiment and criterion but the absolute agreement is poor in both cases. The criterion has also been applied to the

test results for this type of flutter with follow up ratio N = ±3 and as the experimental results for these cases do not differ significantly from those for N = 0 the same general conclusions concerning agreement apply. If we restrict further consideration to the Method 4 derivative case then an improvement in the agreement is obtained if we use a frequency weighting factor B = 1/10, the criterion curve being widened somewhat. From Table 6 it can be seen that this change in frequency weighting factor may be justified as the overall agreement with the measured flutter frequencies is improved. In view of the fact that the agreement was still poor in the negative range of X it was decided to try a further variation in weighting factor and a value of B = 100 was considered. The coefficient of X in the criterion equation is no longer insignificant. A skewed criterion curve results which is shown in Fig.28. Most of the flutter points now lie within the curve in the central range of X but the shape of the curve is completely different from the experimental ones. The flutter frequencies using this approximation are shown in Table 6 and they are in very poor agreement with the measured values. From this point of view there seems to be little justification for using this weighting approximation.

The calculations indicate that the flutter is of a ternary type involving aileron motion which reduces the binary speed although the frequency is unaffected. It is to be expected that the agreement will be worse in this case where we are using a criterion based on the assumption of binary type flutter in order to predict the ternary bounds.

Application of the basic criterion to aileron-tab flutter for three values of aileron frequency is shown in Fig.29, the follow up ratio being zero. The agreement between the experimental results and the criterion using Method 4 derivatives is a good deal better than using Method 2. We shall restrict further discussion to this case. Over the central range of X the majority of the experimental points lie within or very close to the criterion curve and the experimental curves have similar shapes to that of the criterion. Minimum flutter speeds found in practice are of the same order as those predicted by the criterion. The comparison in Table 7 shows that there would be little point in attempting to improve the agreement by making adjustments to the frequency weighting factor for the best agreement with the measured flutter frequencies is obtained with B = 1.

The application of the basic criterion to aileron-tab flutter for three wing-aileron connecting springs when N = +3 is shown in Fig.30. In this instance the criterion curve is defined by the full quadratic equation, including the term in X, which accounts for the skewed form. Over the central range of X the criterion curve exhibits the same trend as the experimental results and the agreement for flutter speed is quite good. Method 4 derivatives lead to slightly the better agreement for the weakest connecting spring case whilst for stiffer connecting springs both methods give conservative estimates of the flutter bounds.

3.3.1 Discussion

In para.3.3 it is shown that it is possible to modify the basic criterion by applying a weighting factor B in the frequency approximation so that there is a better degree of agreement with the experimental flutter speed results than the basic criterion gives. To achieve this improvement the weighting factors that have been found necessary for the systems studied (N = 0) are:-

(1) Wing roll-aileron rotation flutter. B = 0.1. The use of this factor is well justified on the grounds of the improved flutter frequency approximation.

(2) Aileron rotation-tab rotation flutter. B = 1.0. No modification required.

(3) Wing roll-tab rotation flutter. (a) B = 0.1. The use of this factor may be justified on the grounds of the improved frequency approximation. (b) B = 100. The curve defined by this value of B includes most of the experimental points over the central range of X but the use of this factor cannot be justified on frequency grounds. We have noticed that there is doubt about whether the criterion should be applied to this particular case and this should be borne in mind when considering the two widely different values of B at 3(a) and 3(b) above.

The use of the large value of B (= 100) leads to an extremely simple form for the flutter frequency approximation virtually dependent on the frequency of the second mode only so that $\omega^2 = \omega_2^2 + \frac{C_{22}}{A_{22}}\left(\frac{V}{c}\right)^2$ and it was decided to investigate the criterion form that resulted from this approximation. It is interesting to note that Pugsley[12] suggested this form as a possible approximation to the binary wing flexure-torsion flutter frequency. A derivation of this approximation is given in the Appendix. It is shown there that the basic flutter determinant on expansion using this approximation becomes:-

$$\left\{Y + \left(\frac{c_{22}}{a_{22}} - \frac{c_{12}}{a_{12}}\right)\left(\frac{V}{\omega_1}\right)^2\right\}\left\{Y + \left(\frac{c_{22}}{a_{22}} - \frac{c_{21}}{a_{12}}\right)\left(\frac{V}{\omega_1}\right)^2\right\} = 0 \qquad (5)$$

where $Y = \left(\frac{\omega_2}{\omega_1}\right)^2$.

If $\left\{\frac{V}{\omega_1}\right\}^2$ is plotted against Y, the equation reduces to two straight lines. Flutter is possible in the area bounded by these two lines. In most binary systems one of these lines will have positive slope whereas the other will have negative. Points between the latter line and the line Y = 0 are not compatible with a real physical system.

A possible simplified criterion may be formulated which states that the area in which flutter may occur will be bounded by the two lines defined by equation (5) providing that these are of positive slope. Should the slope of either line prove to be negative then the line Y = 0 should replace it as a criterion bound. A right hand bound for Y beyond which flutter will not occur is defined approximately on the basis of the experimental results of this paper by the line $Y = 1.12 + \frac{1.56}{\omega_1}$. When using this criterion form for a particular

binary system, the ratios of aerodynamic to inertia coefficients in equation (5) above are replaced by the same simplified ratios that Molyneux adopts for the corresponding binary cases.

The results of the application of this criterion to the binary flutter cases we have studied is shown in Figs.31-34. For all these cases we are replacing the second boundary lines, which have negative slope, by the lines Y = 0. In the case of aileron-tab flutter (N = 0), Fig.31, most of the experimentally obtained flutter points lie within the bounds predicted by the criterion. Method 4 derivatives lead to better agreement than Method 2. The greatest variation from the criterion bounds is for an aileron frequency of 5.9 c.p.s. where values of $\left(\frac{V}{\omega_1}\right)^2$ for values of Y > 1 are much lower than the criterion would predict.

Fig.32 shows the application of the criterion to the wing roll-tab rotation flutter (N = 0) and it can be seen that the criterion bounds predict the area in which flutter occurs quite well. The Method 4 derivatives yield a somewhat better agreement to the minimum flutter speeds than the other set.

The results for wing roll-aileron rotation flutter (N = -3) are shown in Fig.33. Method 4 and Method 2 derivatives lead to good agreement for the flutter boundary.

Fig.34 shows the application to aileron rotation-tab rotation flutter (N = +3). No limiting values of Y can be assigned in this case as the aileron frequency varies along each of the curves. The aileron frequency corresponding to any point on the curves of the figure depends on the particular tab spring fitted. Method 4 derivatives yield flutter boundaries that are in good agreement with the experimental bounds. The order of agreement between the measured flutter speeds and the boundary values is of the same order as that between the measured speeds and the original criterion bound (Fig.30).

To summarise, one may say that this criterion form provides a reasonable approximation to the flutter bounds for the types of flutter that have been studied. The flutter frequencies obtained with the "single frequency" approach are shown in Tables 5-7, and they are in poor agreement with the measured values so that from this aspect the criterion form is difficult to justify. Method 4 derivatives lead to better agreement for the flutter boundaries.

4 CONCLUSIONS

Flutter tests have been made on a wing-aileron-tab system in which the effects of variation in the following parameters have been investigated. (a) Main surface natural frequency in roll (b) Control surface natural frequency in rotation (c) Tab natural frequency in rotation and (d) Follow up ratio.

Four flutter modes of oscillation of the system were found depending on the values of the above parameters and these were the ternary and the three binary types. The results provide a general indication of the behaviour that may be expected with a practical wing-aileron-tab system in which the main

surface motion is in the fundamental bending mode. They may not, however, be applied directly to predict the flutter characteristics of such a system.

Supporting calculations have been made using sets of aerodynamic derivatives based on (1) measured steady motion derivatives for this wing, (2) oscillatory derivative measurements on this and a similar two-dimensional wing and (3) predicted steady motion derivatives. The calculations showed that this last set gave the best overall guide to the flutter characteristics of the system but the first set gave a better agreement with experiment for the free aileron case at low rolling stiffness. In general the calculations led to unconservative estimates of flutter speed; the calculated flutter speeds were in poorest agreement when the measured speeds were very low.

A comparison has been made between the experimental results and the predictions of the latest flutter criteria. It has been found that by applying weighting factors (B) in the basic frequency assumption on which the criteria depend, tolerable agreement between the experimental results and the criteria can be obtained. The basic frequency approximation is

$$\omega^2 = \frac{1}{1+B}\left\{\omega_1^2 + \frac{C_{11}}{A_{11}} V_c^2 + B\left(\omega_2^2 + \frac{C_{22}}{A_{22}} V_c^2\right)\right\}$$

and a value of B = 1 was considered appropriate when the criterion was first proposed. For the flutter types found in this investigation the values of B that led to the best degree of agreement for flutter speed were:-

(1) Wing roll-aileron rotation flutter, B = 0.1.

(2) Aileron rotation-tab rotation flutter, B = 1.0.

(3) Wing roll-tab rotation flutter, B = 100. (This value of B was the best conservative value for the determination of flutter speed, although a value of 0.1 yielded improved frequency approximations.)

A further investigation has been made of a criterion form depending on a flutter frequency approximation based on the frequency of one of the uncoupled modes of a binary system. The flutter regions found in practice all lay essentially within the bounds predicted by this form.

ACKNOWLEDGMENTS

The author wishes to express his thanks to Mr. W.G. Molyneux, Structures Department, R.A.E. who designed the rig and model and to acknowledge the assistance given at various stages of the work by Messrs. W.A. Coles and B.W. Barber, both formerly of Structures Department, R.A.E.

REFERENCES

No.	Author	Title, etc.
1	Collar, A.R., Sharpe, G.D.	A criterion for the prevention of spring-tab flutter. A.R.C. R.& M. 2637. June, 1946.
2	Wittmeyer, H.	Theoretical investigations of ternary lifting surface - control surface - trimming tab flutter and derivation of a flutter criterion. A.R.C. R.& M. 2671. October, 1948.
3	Wittmeyer, H., Templeton, H.	Criteria for the prevention of flutter of tab systems. A.R.C. R.&.M. 2825. January, 1950.
4	Hall, H.	The effect of wing torsion on aileron-tab flutter. A.R.C. R.&.M. 3072. April, 1956.
5	Guyett, P.R.	Empirical values of derivatives. Chapter 11, Part 2, AGARD Manual of Aeroelasticity. 1961.
6	Molyneux, W.G.	Design criteria and approximate formulae. Chapter 6, Part 5, AGARD Manual of Aeroelasticity. 1961.
7	Lyons, D.J., Bisgood, P.L.	An analysis of the lift slopes of airfoils of small aspect ratio including fins with design charts for aerofoils and control surfaces. A.R.C. R.& M. 2308. January, 1945.
8	Walker, J.G.	Note on the rapid estimation of the low speed hinge moments of unbalanced unswept controls. A.R.C. 15231. August, 1952.
9	Molyneux, W.G., Ruddlesden, F.	Derivative measurements and flutter tests on a rectangular wing with a full span control surface oscillating in modes of wing roll and aileron rotation. A.R.C. R.& M. 3010. February, 1955.
10	Wight, K.C.	Measurements of two-dimensional derivatives on a wing-aileron-tab system with a 1541 section aerofoil. A.R.C. R.& M. 3029. March, 1955.
11	Minhinnick, I.T.	Aerodynamic derivatives. Paper 4 of "A Symposium on the flutter problem in aircraft design". R.A.E. Report Structures 147, May 1953.
12	Pugsley, A.G.	A simplified theory of wing flutter. A.R.C. R.& M. 1839. April, 1937.

MAIN SYMBOLS

N = Follow up ratio and is defined as the ratio of tab angle to aileron angle when the aileron is rotated with the tab control lever held fixed

V_c = Flutter speed

ω_R = Wing natural frequency in roll

ω_A = Aileron natural frequency

ω_T = Tab natural frequency

ω_1, ω_2 = Uncoupled natural frequencies of a pair of modes

A_{11}, A_{22} = Structural inertia coefficients of the two modes

C_{11}, C_{22} = Aerodynamic stiffness coefficients of the two modes

APPENDIX 1

DERIVATION OF AN APPROXIMATION TO THE FLUTTER FREQUENCY OF A BINARY SYSTEM AND ITS USE IN FORMULATING A SIMPLE FLUTTER CRITERION

The flutter determinant may be written as

$$\begin{vmatrix} a_{11}\lambda^2 + b_{11}\lambda + c_{11} + e_{11} , & a_{12}\lambda^2 + b_{12}\lambda + c_{12} \\ a_{12}\lambda^2 + b_{21}\lambda + c_{21} , & a_{22}\lambda^2 + b_{22}\lambda + c_{22} + c_{22} \end{vmatrix} = 0$$

Expanding as a polynomial in λ we have

$$p_o \lambda^4 + p_1 \lambda^3 + p_2 \lambda^2 + p_3 \lambda + p_4 = 0$$

where

$$p_o = (a_{11} a_{22} - a_{12}^2)$$

$$p_1 = a_{11} b_{22} + a_{22} b_{11} + a_{12} b_{21} + a_{12} b_{12}$$

$$p_2 = a_{11}(c_{22} + e_{22}) + b_{11} b_{22} + a_{22}(c_{11} + e_{11}) - a_{12} c_{21} - b_{12} b_{21} - a_{12} c_{12}$$

$$p_3 = b_{11}(c_{22} + e_{22}) + b_{22}(c_{11} + e_{11}) - b_{21} c_{12} - b_{12} c_{21}$$

$$p_4 = (c_{11} + e_{11})(c_{22} + e_{22}) - c_{12} c_{21}$$

Writing $\lambda = i\nu$ then the imaginary part of the equation gives

$$\nu^2 = \frac{p_3}{p_1} = \frac{b_{11}(c_{22} + e_{22}) + b_{22}(c_{11} + e_{11}) - b_{21} c_{12} - b_{12} c_{21}}{a_{11} b_{22} + a_{22} b_{11} + a_{12} b_{21} + a_{12} b_{12}}$$

and if we assume that the ratios $\frac{b_{12}}{b_{11}}$, $\frac{b_{21}}{b_{11}}$, $\frac{b_{22}}{b_{11}}$ are sufficiently small so that they may be neglected then

$$\nu^2 = \frac{c_{22} + e_{22}}{a_{22}} \quad \text{where} \quad e_{22} = \frac{a_{22}\,\omega_2^2\,c^2}{V^2}$$

or

$$\omega^2 = \omega_2^2 + \frac{c_{22}}{a_{22}}\left(\frac{V}{c}\right)^2 .$$

The real part of the equation is

$$(a_{11}a_{22} - a_{12}^2)\nu^4 - \left[a_{11}(c_{22}+e_{22}) + b_{11}b_{22} + a_{22}(c_{11}+e_{11}) - a_{12}c_{21} - b_{12}b_{21} - a_{12}c_{12}\right]\nu^2$$
$$+ (c_{11}+e_{11})\,(c_{22}+e_{22}) - c_{12}c_{21} \;=\; 0$$

and making use of the expression for frequency parameter ν and with the assumption above about dampings

$$(a_{11}a_{22} - a_{12}^2)\left\{\frac{c_{22}+e_{22}}{a_{22}}\right\}^2 - \left[a_{11}(c_{22}+e_{22}) + a_{22}(c_{11}+e_{11}) - a_{12}c_{21} - a_{12}c_{12}\right]$$
$$\left\{\frac{c_{22}+e_{22}}{a_{22}}\right\} + (c_{11}+e_{11})\,(c_{22}+e_{22}) - c_{12}e_{21} \;=\; 0$$

or $$-a_{12}^2(c_{22}+e_{22})^2 - \left[a_{22}^2(c_{11}+e_{11})\,(c_{22}+e_{22}) - a_{12}(c_{12}+c_{21})\,(c_{22}+e_{22})a_{22}\right]$$
$$+\left[(c_{11}+e_{11})\,(c_{22}+e_{22}) - c_{12}c_{21}\right]a_{22}^2 \;=\; 0$$

or $$-a_{12}^2\left(c_{22} + \frac{a_{22}\,\omega_2^2\,c^2}{V^2}\right)^2 + a_{12}\,(c_{12}+c_{21})\,a_{22}\left(c_{22} + \frac{a_{22}\,\omega_2^2\,c^2}{V^2}\right)$$
$$- c_{12}\,c_{21}\,a_{22}^2 \;=\; 0$$

after some reduction this becomes

$$-a_{12}^2\left(\frac{\omega_2}{\omega_1}\right)^4 + \left[-2\,a_{12}^2\,\frac{c_{22}}{a_{22}} + a_{12}\,(c_{12}+c_{21})\right]\left(\frac{V}{\omega_1 c}\right)^2\left(\frac{\omega_2}{\omega_1}\right)^2$$
$$+\left[-a_{12}^2\left(\frac{c_{22}}{a_{22}}\right)^2 + \frac{a_{12}}{a_{22}}\,(c_{12}+c_{21})\,c_{22} - c_{12}\,c_{21}\right]\left(\frac{V}{\omega_1 c}\right)^4 \;=\; 0\,.$$

Writing $Y = \left(\frac{\omega_2}{\omega_1}\right)^2$, $\frac{V}{c} = v$.

$$Y^2 + \left\{2\frac{c_{22}}{a_{22}} - \left(\frac{c_{12}}{a_{12}} + \frac{c_{21}}{a_{12}}\right)\right\}\left(\frac{v}{\omega_1}\right)^2 Y$$

$$+ \left\{\left(\frac{c_{22}}{a_{22}}\right)^2 - \frac{c_{22}}{a_{12}}\left(\frac{c_{12}}{a_{12}} + \frac{c_{21}}{a_{12}}\right) + \frac{c_{12}}{a_{12}}\frac{c_{21}}{a_{12}}\right\}\left(\frac{v}{\omega_1}\right)^4 = 0$$

and this equation may be factorised

$$\left\{Y + \left(\frac{c_{22}}{a_{22}} - \frac{c_{21}}{a_{12}}\right)\left(\frac{v}{\omega_1}\right)^2\right\}\left\{Y + \left(\frac{c_{22}}{a_{22}} - \frac{c_{12}}{a_{12}}\right)\left(\frac{v}{\omega_1}\right)^2\right\} = 0 .$$

The criterion is based on the above equation.

TABLE 1

Structural details of wing-aileron-tab system (N = 0)

Wing length, roll axis to tip	=	3.04 ft
Wing chord	=	1.5 ft
Wing aspect ratio	=	4.05
Aileron chord aft of H.L. (circular nosed control)	=	5.6 in.
Tab chord aft of H.L. (circular nosed tab)	=	1.4 in.
Thickness : chord ratio	=	0.15
Aileron span	=	17.95 in.
Tab span	=	11.70 in.
Aileron limits (η)	=	0.501 to 1.000
Tab limits (η)	=	0.515 to 0.840

m_r = 1.01 lb/in.

m_A = 0.08806 lb/in.

m_t = 0.01444 lb/in.

k_A = 0.3577

k_t = 0.4638

x_A = 0.1813

x_t = 0.1787

E_A = 0.31

E_t = 0.07

d = 3.0

E_2 = 0.25

where η $\frac{\text{perpendicular distance from roll axis to point on wing}}{\text{wing-span}}$

TABLE 2

Aileron and tab natural frequencies corresponding to particular springs making the wing to aileron and wing to tab connections and for gear ratios of ±3

Wing tab connecting spring	None	1T	2T	3T	4T	5T	6T	7T
Tab frequency (c.p.s.)	0	4.2	5.4	6.5	11.2	13.0	15.3	16.6
Wing aileron connecting spring	Aileron frequencies (c.p.s.)							
None	0	-	-	2.2	3.8	4.4	5.8	7.0
1A	3.6	3.6	3.8	4.0	5.0	5.8	6.6	7.8
2A	5.9	6.0	6.0	6.2	7.0	7.5	8.0	9.2
3A	8.8	8.8	8.8	9.0	9.6	10.0	10.5	11.2
4A	16.2	16.2	16.2	16.2	17.0	17.0	17.2	18.0

TABLE 3

A comparison of the measured and predicted steady motion derivatives

Derivative	Experimental value	Predicted value
ℓ_β	0.6006	0.8953
ℓ_γ	0.2061	0.5043
$(-h_\beta)$	0.01056	0.02253
$(-h_\gamma)$	0.02394	0.03414
$(-t_\gamma)$	0.001209	0.001037

TABLE 4

The oscillatory derivatives obtained by four methods

Derivative	Derivation			
	Measurements by Molyneux[9] and Wight[10] with aspect ratio modification by Method 1	Measurements by Molyneux[9] and Wight[10] with aspect ratio modification by Method 3	Guyett method based on steady motion derivatives measured on this wing Method 2	Guyett method based on predicted steady motion derivatives Method 4
ℓ_β	0.67	0.5436	0.4836	0.7209
$\ell_{\dot\beta}$	0.1439	0.1303	0.1098	0.1637
ℓ_γ			0.1374	0.3362
$\ell_{\dot\gamma}$			0.01621	0.03966
$(-h_\beta)$	0.01722	0.01406	0.008830	0.01884
$(-h_{\dot\beta})$	0.01452	0.01315	0.005996	0.01279
$(-h_\gamma)$	0.02025	0.008722	0.02194	0.03129
$(-h_{\dot\gamma})$	0.002810	0.001844	0.002093	0.002985
$(-t_\gamma)$	0.001294	0.0005054	0.001142	0.0009795
$(-t_{\dot\gamma})$	0.0002941	0.0001930	0.0002179	0.0001869

On the basis of Molyneux's work (Ref.9) the derivatives have been taken to be constant with frequency parameter over the range covered by the flutter tests. The average values of frequency parameter (based on wing chord) occurring in the three binary types of flutter found were:-

wing roll - aileron rotation 1.1

aileron rotation - tab rotation 1.5

wing roll - tab rotation 2.5

TABLE 5

A comparison of the measured flutter frequencies for wing aileron flutter (N = 0) with those predicted by the criterion approximations, Method 4 derivatives

Aileron frequency c.p.s.	Wing rolling frequency c.p.s.	Flutter frequency c.p.s.	Frequency approximation B = 1 c.p.s.	Frequency approximation B = 0.1 c.p.s.	"Single frequency" approximation c.p.s.
0	1.1	1.08	0.9	1.07	0.63
	3.5	3.5	2.8	3.4	1.8
	5.6	5.4	4.6	5.4	3.4
3.6	3.5	3.7	3.8	3.6	4.1
	5.6	5.6	5.0	5.5	4.3

TABLE 6

A comparison of the measured flutter frequencies for wing tab flutter (N = 0) with those predicted by the criterion approximations, Method 4 derivatives

Rolling frequency c.p.s.	Tab frequency c.p.s.	Flutter frequency c.p.s.	Frequency approxi-mation B = 1 c.p.s.	Frequency approxi-mation B = 0.1 c.p.s.	Frequency approxi-mation B = 100 c.p.s.	"Single frequency" approxi-mation c.p.s.
5.6	0	5.4	4.8	5.5	3.9	3.9
	2	5.5	4.9	5.5	4.0	4.0
	4	5.6	5.2	5.6	5.2	5.2

TABLE 7

A comparison of the measured flutter frequencies for aileron tab flutter (N = 0) with those predicted by the criterion approximations, Method 4 derivatives

Aileron frequency c.p.s.	Tab frequency c.p.s.	Flutter frequency c.p.s.	Frequency approximation B = 1 c.p.s.	Frequency approximation B = 0.1 c.p.s.	"Single frequency" approximation c.p.s.
	2	7.5	7.4	8.9	5.1
8.8	6	8.8	7.9	8.8	6.7
	10	11.0	9.7	9.0	10.4
	4	5.7	5.2	5.9	4.4
5.9	6	6.6	6.1	6.0	6.2
	8	7.7	7.5	6.4	8.6

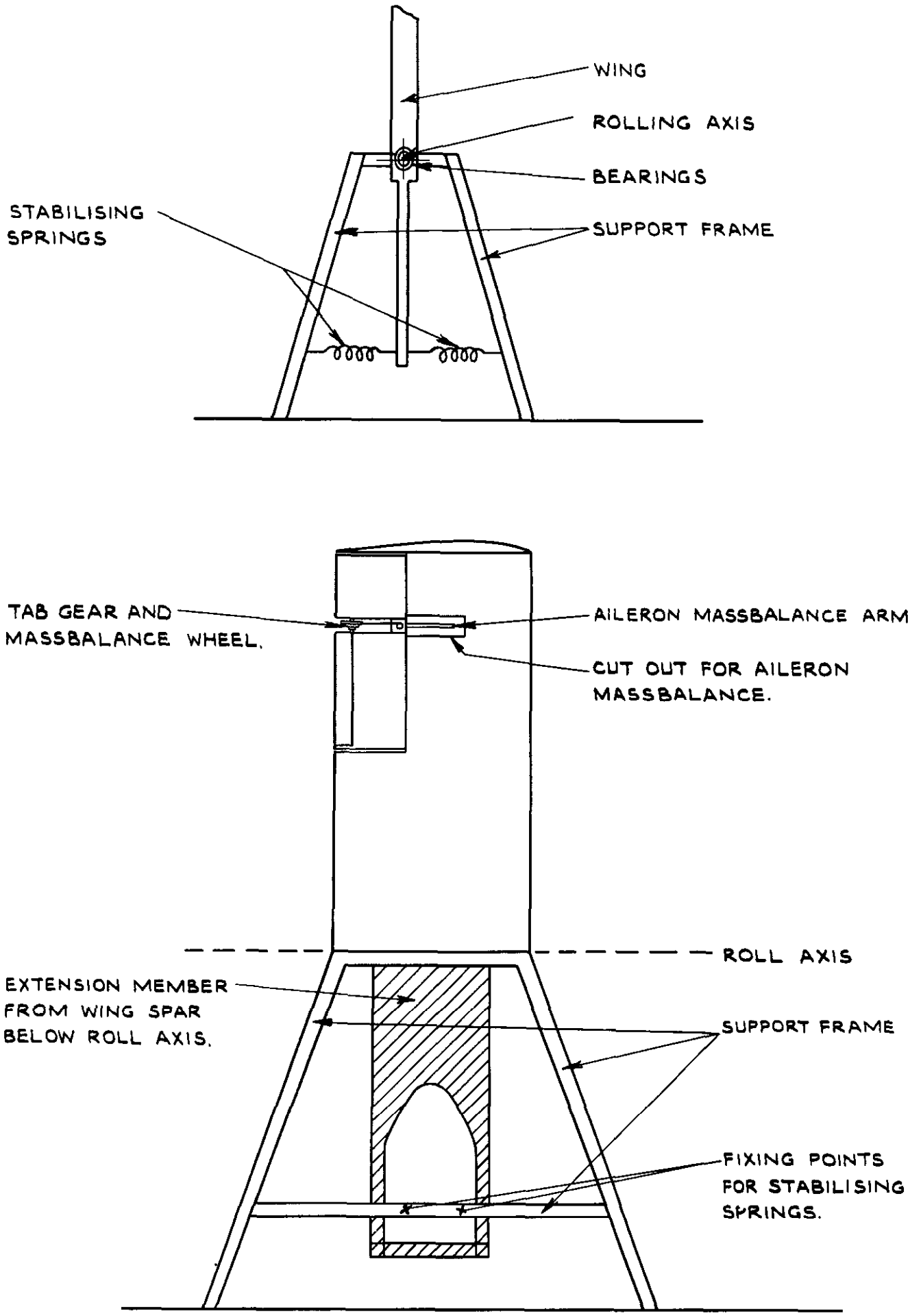

FIG.1 ARRANGEMENT OF THE FLUTTER RIG AND MODEL.

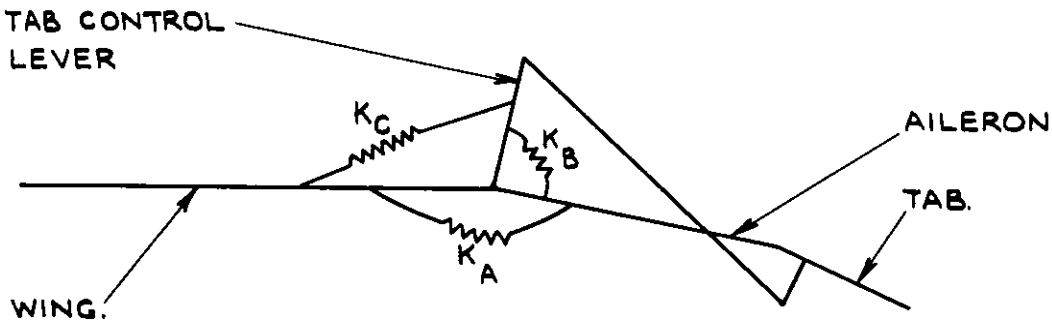

FIG.2. THE SPRING CONNECTIONS GOVERNING AILERON & TAB MOTION.

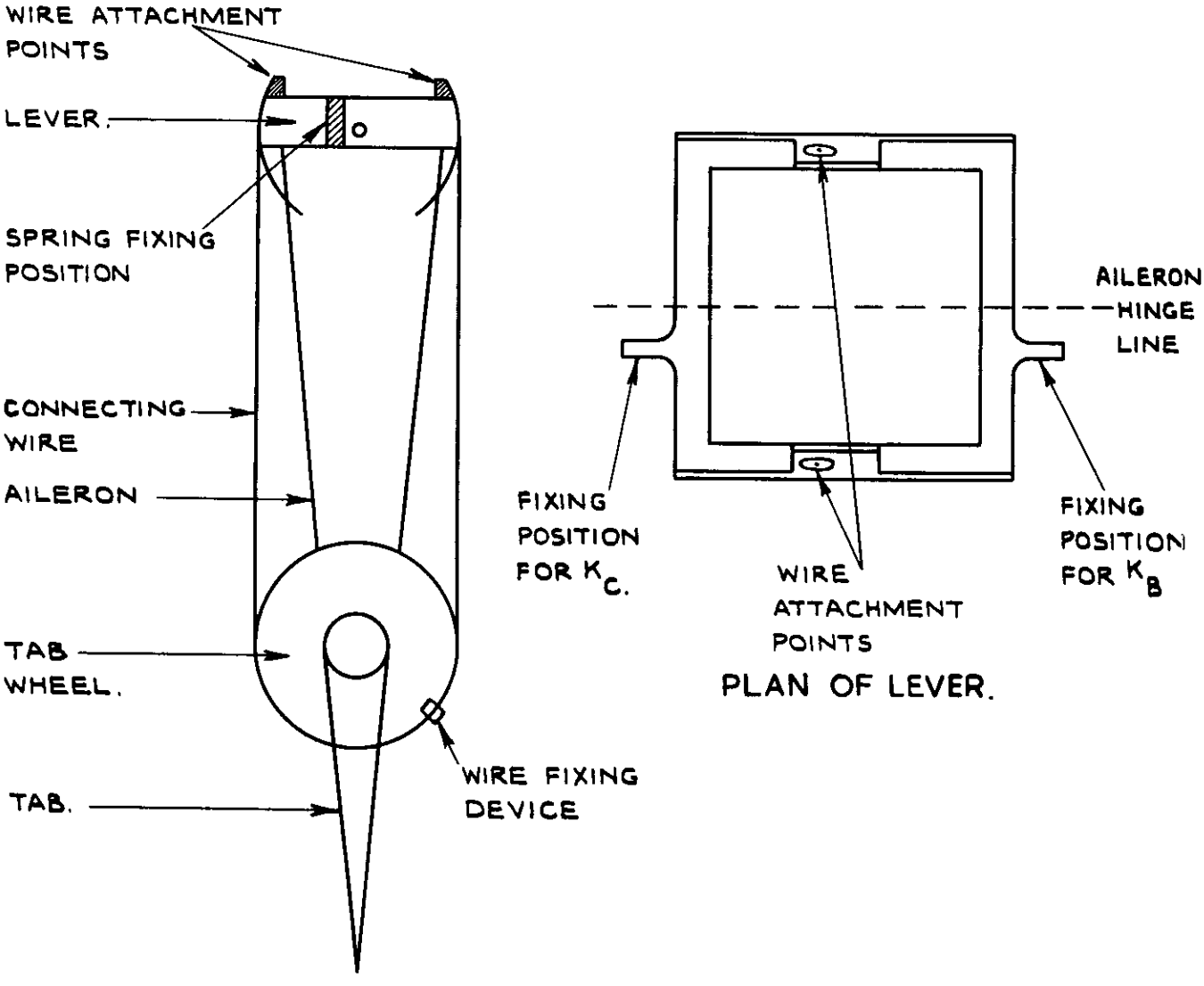

FIG 3 ILLUSTRATION OF THE ARRANGEMENT OF THE TAB GEARING SYSTEM.

N = O

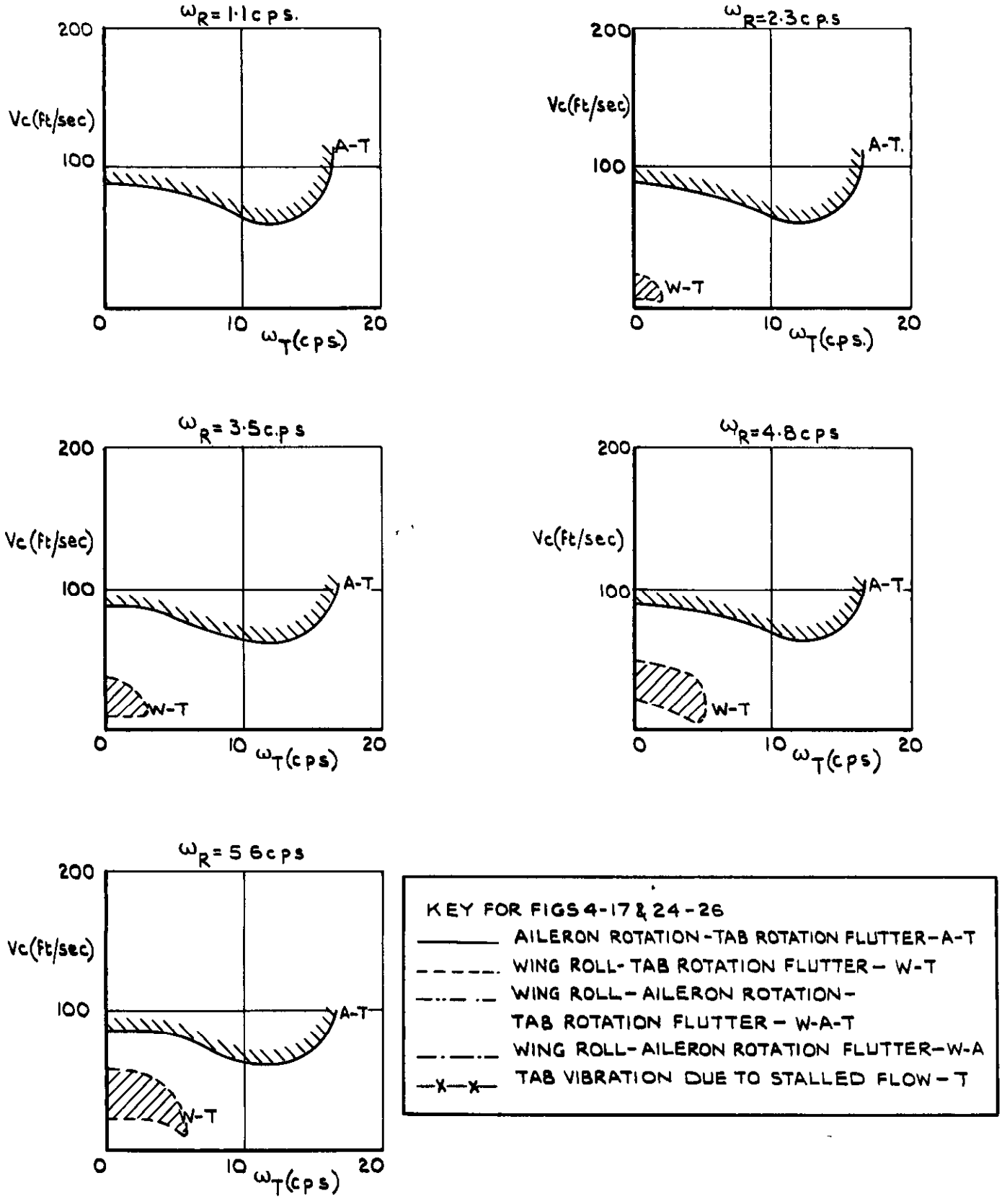

TRIMMING TAB

FIG.4. THE VARIATION OF FLUTTER SPEED WITH TAB FREQUENCY FOR SEVERAL VALUES OF WING ROLLING FREQUENCY AND CONSTANT AILERON FREQUENCY OF 16·2 C.P.S.

N = O

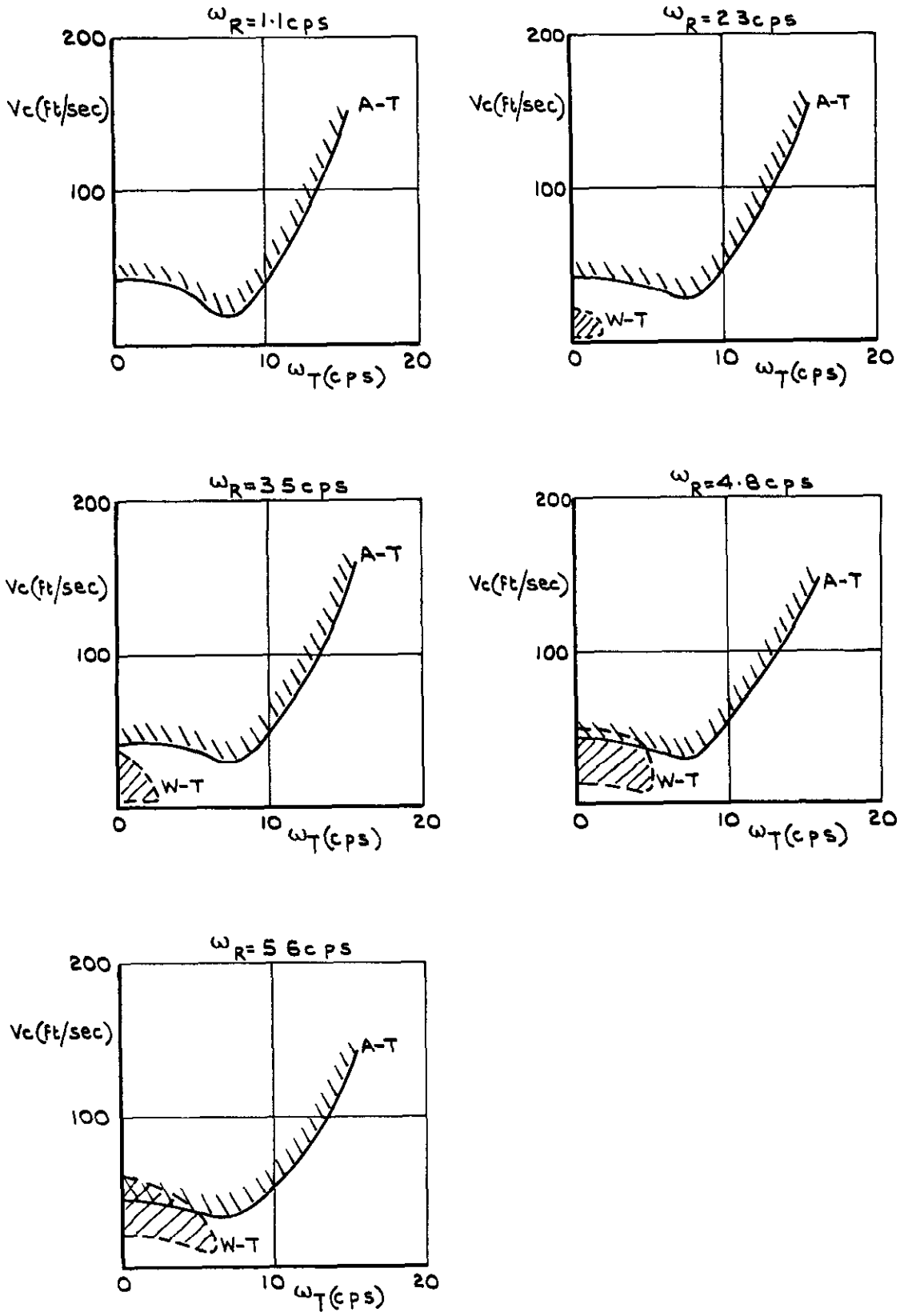

TRIMMING TAB

FIG. 5. THE VARIATION OF FLUTTER SPEED WITH TAB FREQUENCY FOR SEVERAL VALUES OF WING ROLLING FREQUENCY AND CONSTANT AILERON FREQUENCY OF 8·8 C.P.S

N = O

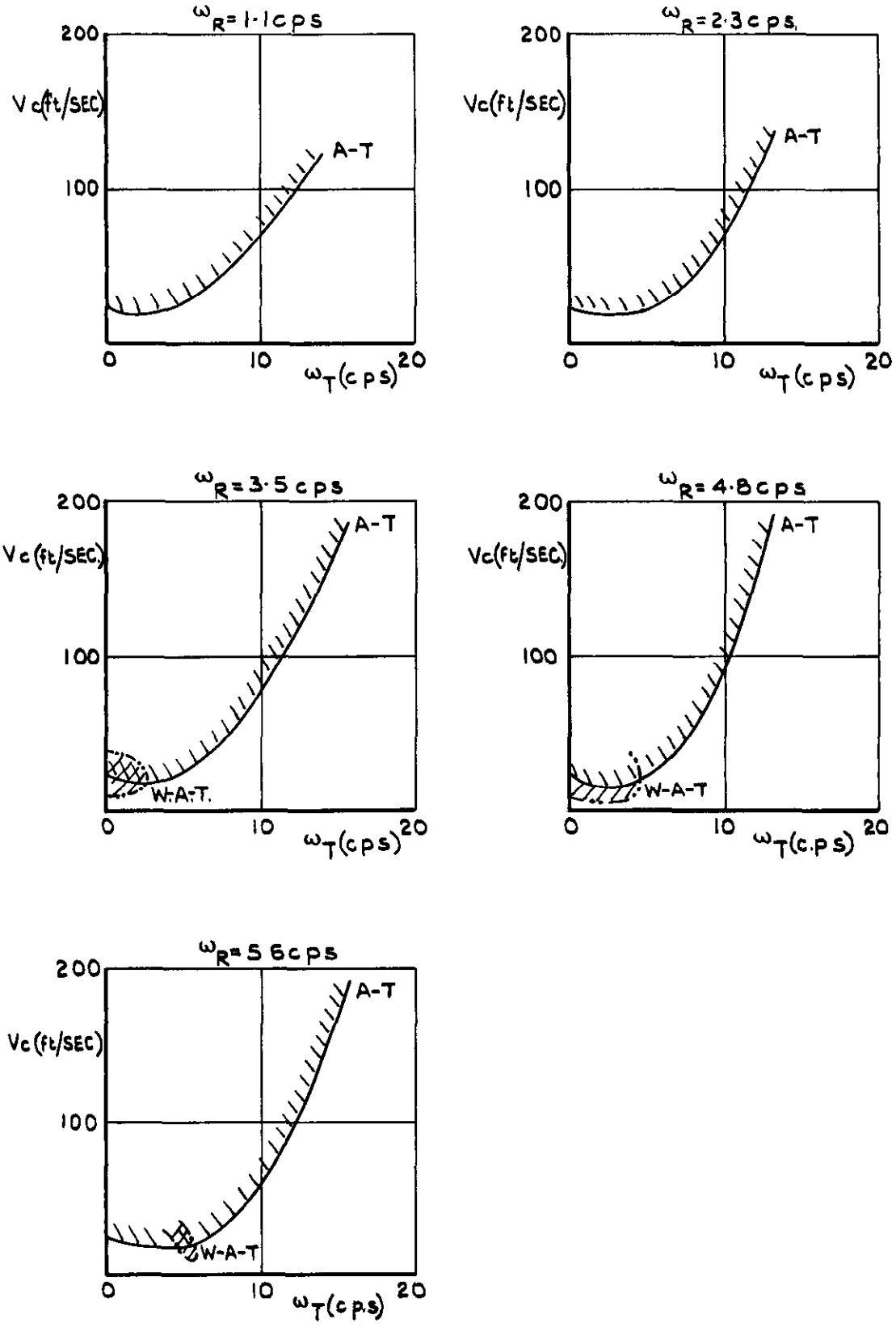

TRIMMING TAB

FIG. 6 THE VARIATION OF FLUTTER SPEED WITH TAB FREQUENCY FOR SEVERAL VALUES OF WING ROLLING FREQUENCY AND CONSTANT AILERON FREQUENCY OF 5·9 C.P.S.

N = O

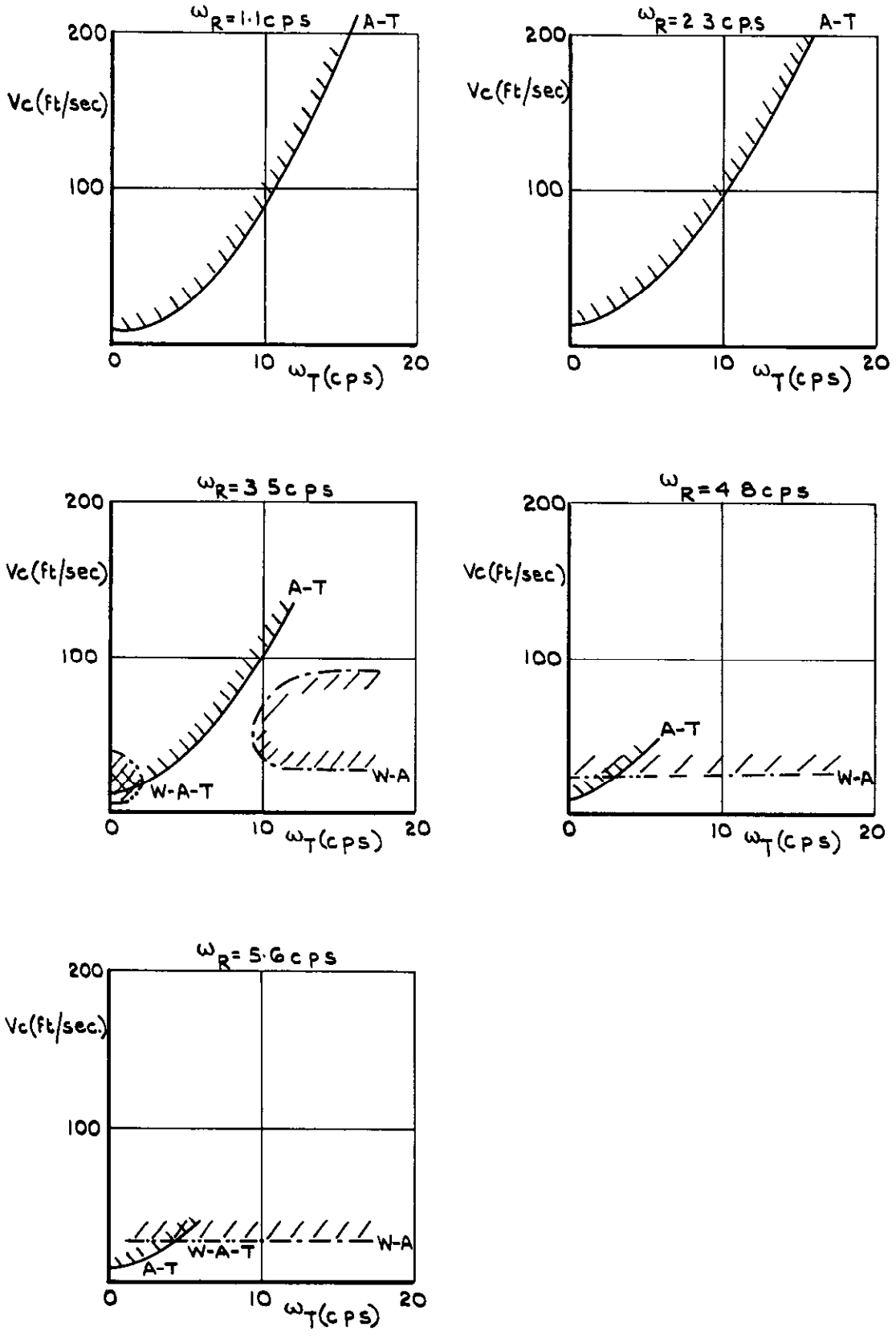

TRIMMING TAB

FIG. 7. THE VARIATION OF FLUTTER SPEED WITH TAB FREQUENCY FOR SEVERAL VALUES OF WING ROLLING FREQUENCY AND CONSTANT AILERON FREQUENCY OF 3·6 C.P.S.

N = O.

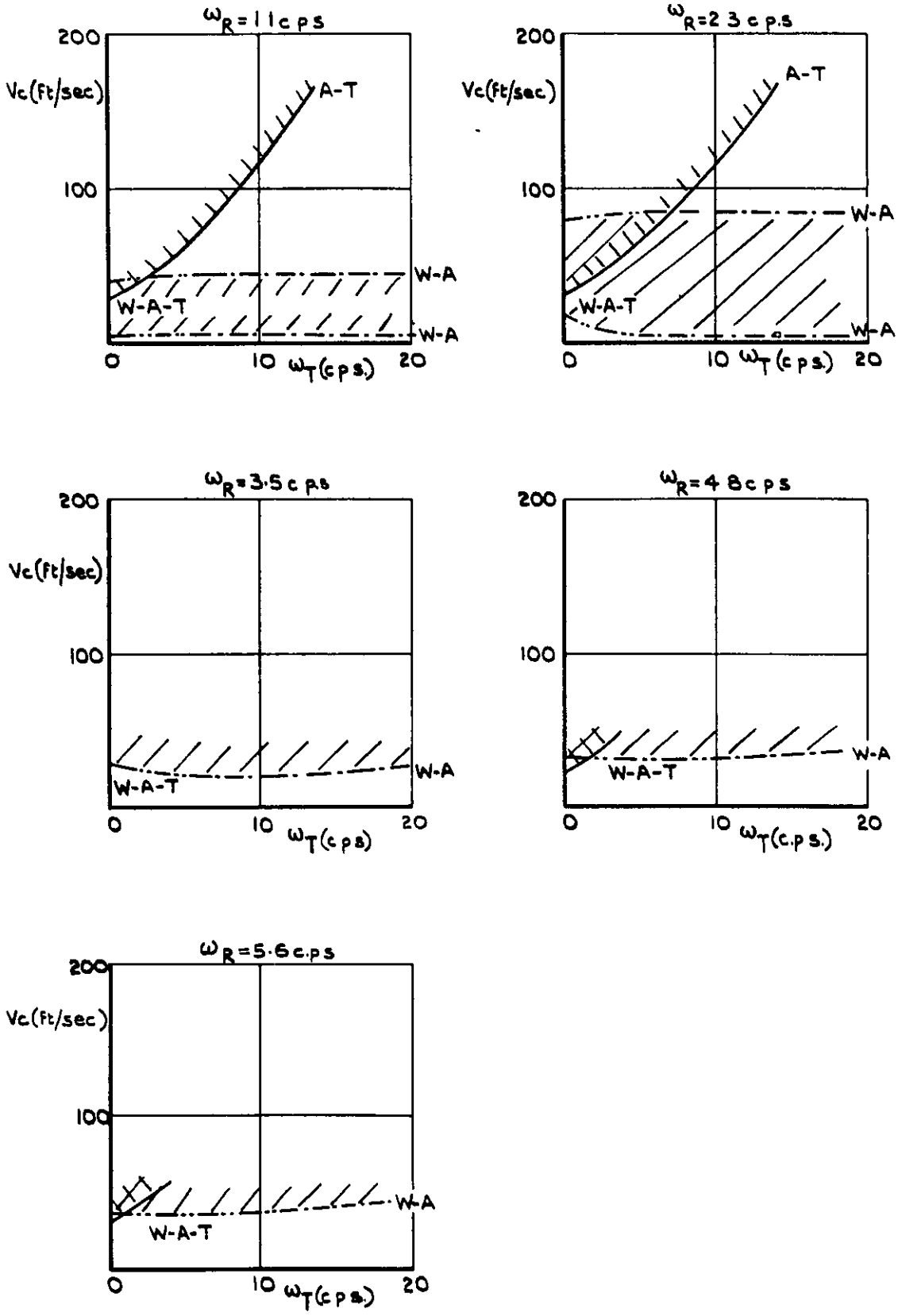

TRIMMING TAB

FIG. 8. THE VARIATION OF FLUTTER SPEED WITH TAB FREQUENCY FOR SEVERAL VALUES OF WING ROLLING FREQUENCY AND FREE AILERON.

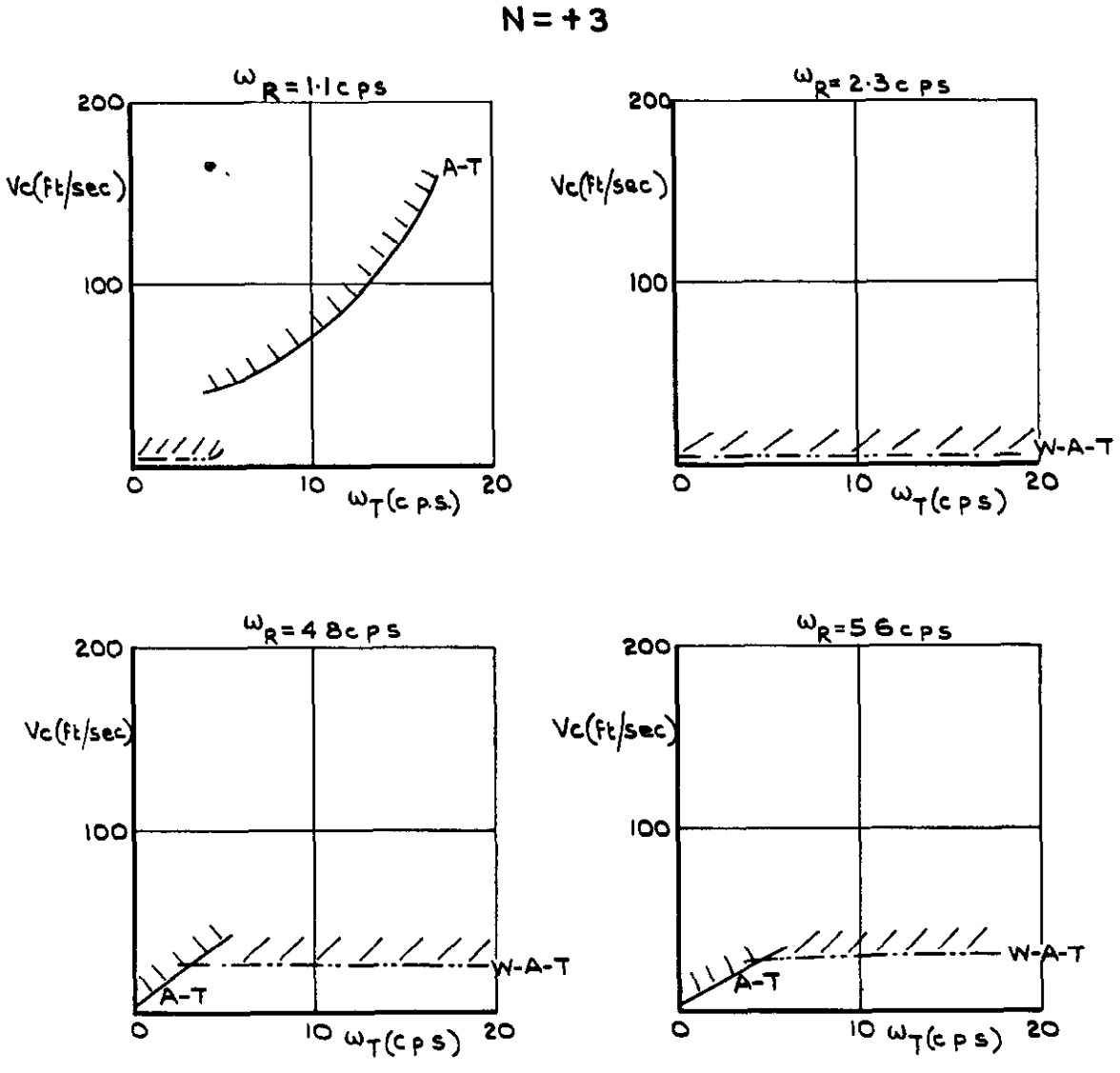

FIG. 9. THE VARIATION OF FLUTTER SPEED WITH TAB FREQUENCY FOR SEVERAL VALUES OF WING ROLLING FREQUENCY & WITH NO AILERON CONNECTING SPRING.

N = + 3

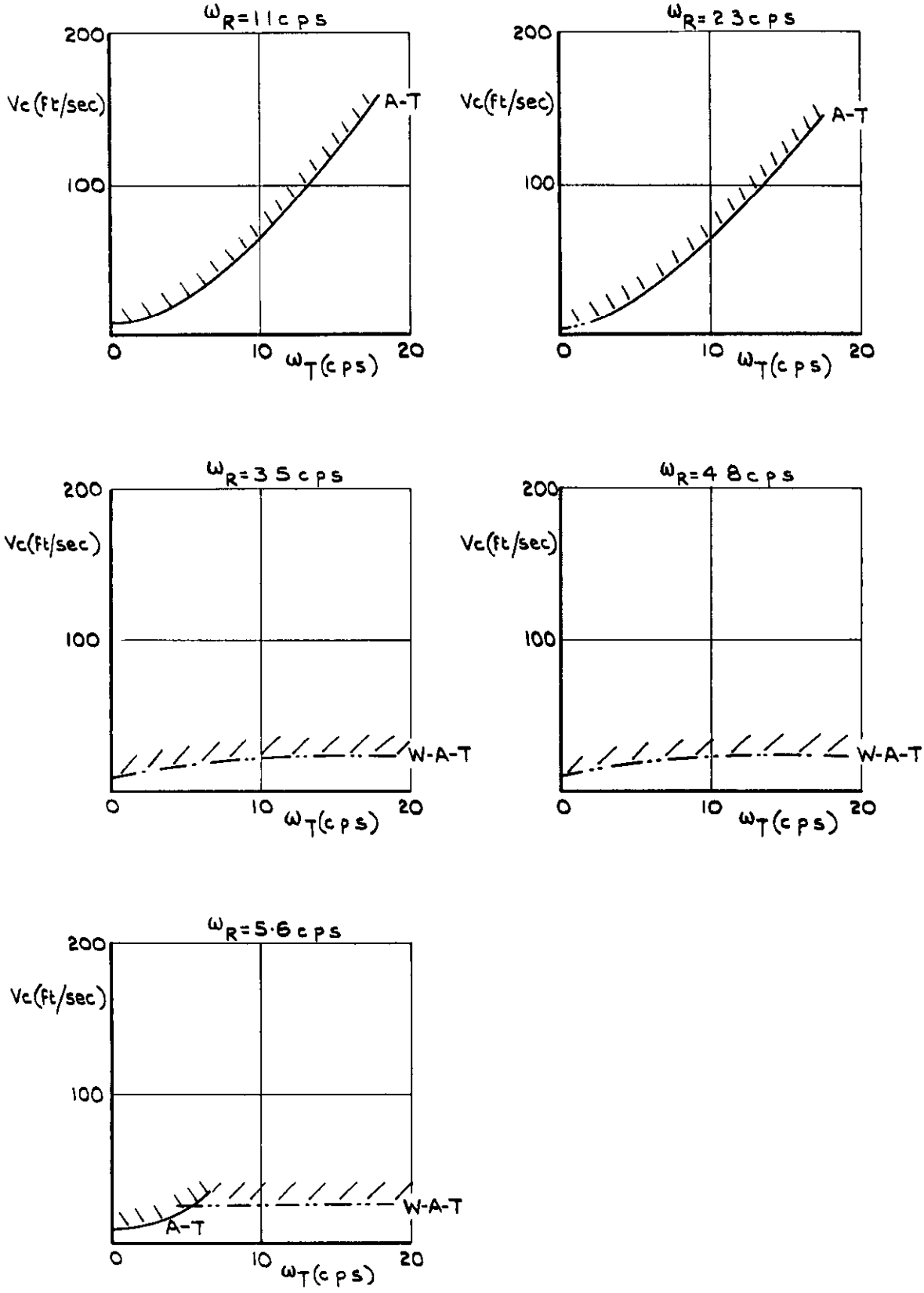

GEARED TAB

FIG. 10. THE VARIATION OF FLUTTER SPEED WITH TAB FREQUENCY FOR SEVERAL VALUES OF WING ROLLING FREQUENCY & WITH No. 1A AILERON CONNECTING SPRING FITTED.

N = +3

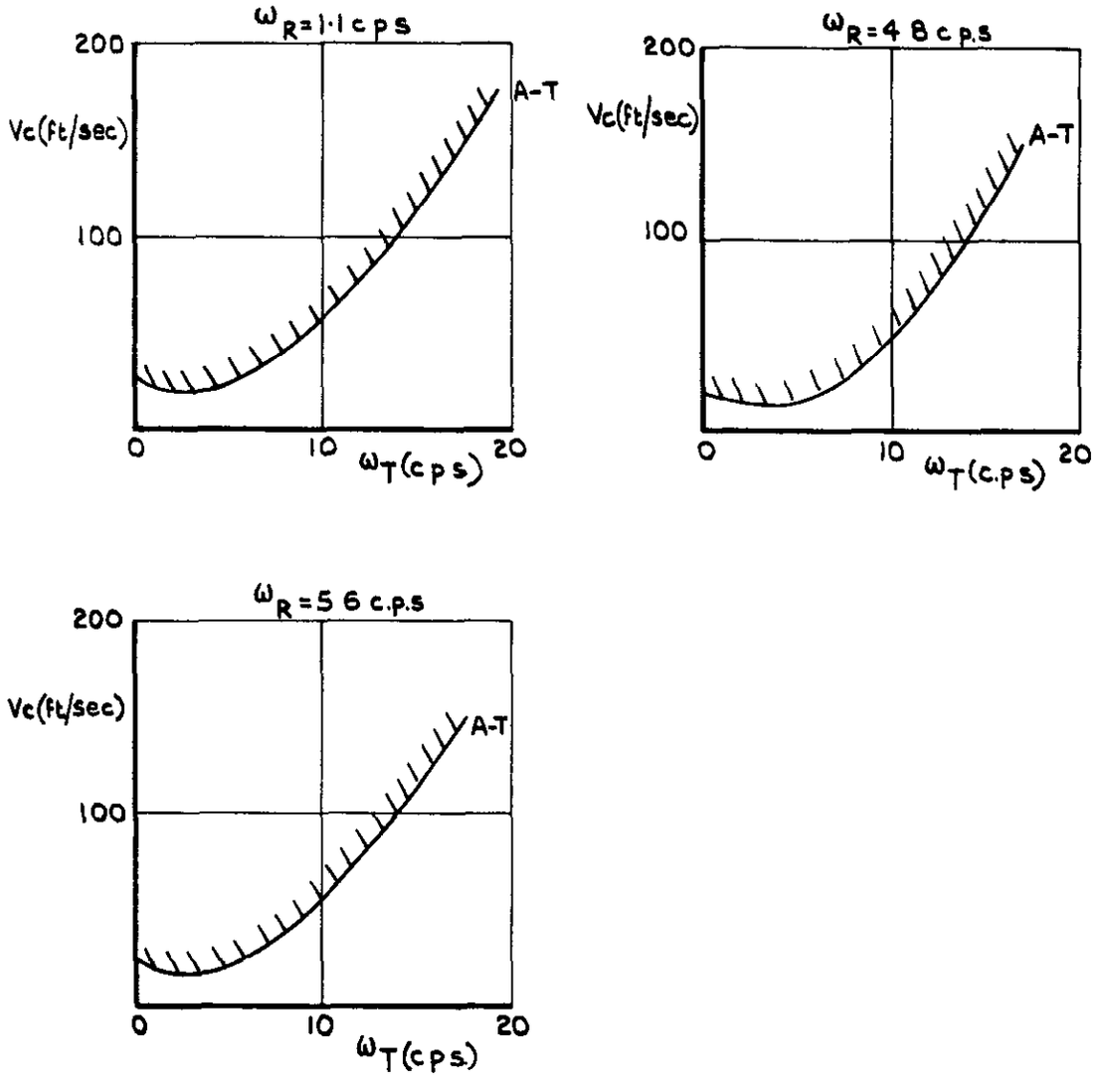

GEARED TAB

FIG. 11. THE VARIATION OF FLUTTER SPEED WITH TAB FREQUENCY FOR SEVERAL VALUES OF WING ROLLING FREQUENCY & WITH No. 2A AILERON CONNECTING SPRING FITTED.

N = +3

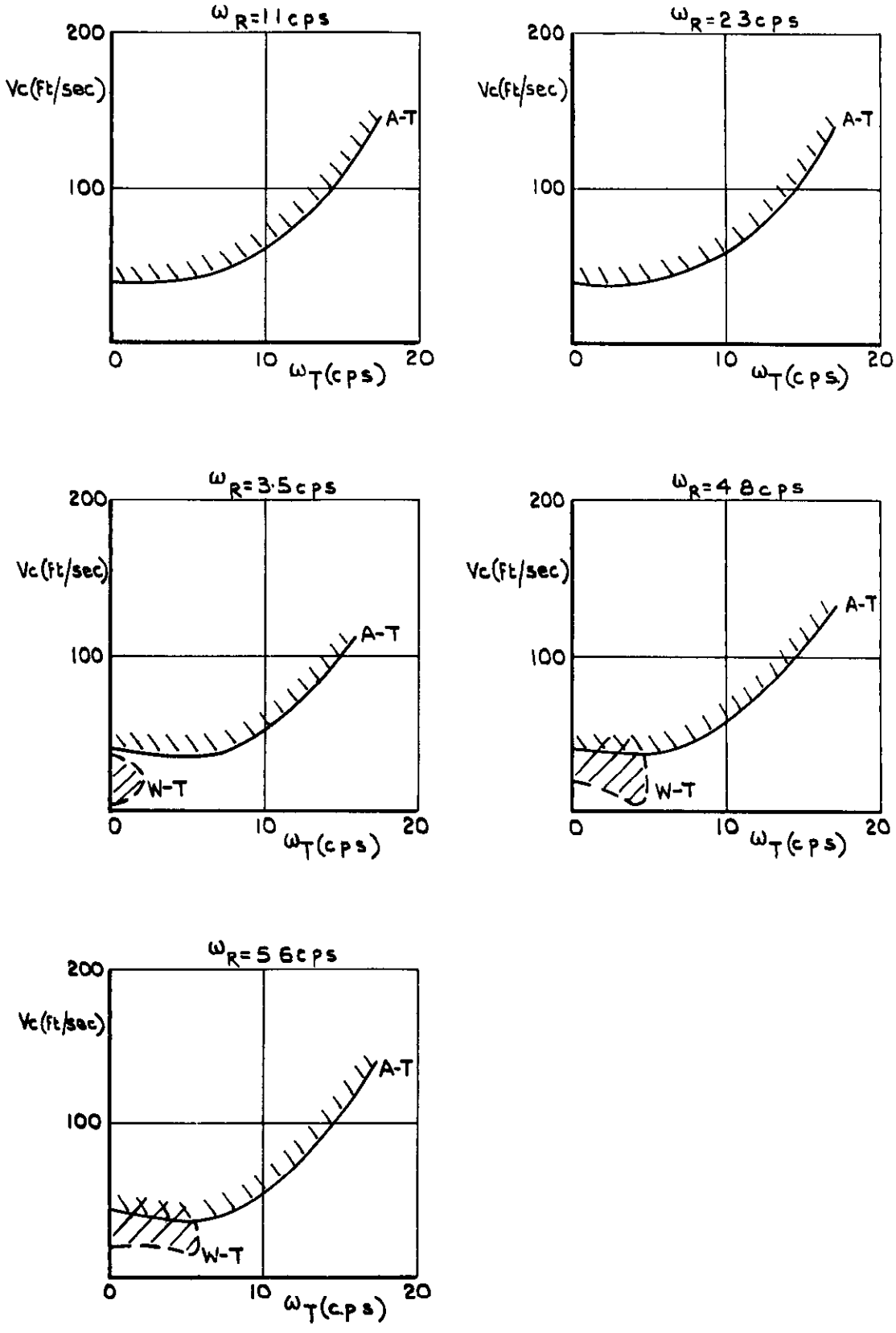

GEARED TAB

FIG. 12. THE VARIATION OF FLUTTER SPEED WITH TAB FREQUENCY FOR SEVERAL VALUES OF WING ROLLING FREQUENCY & WITH No. 3A AILERON CONNECTING SPRING FITTED.

N = +3

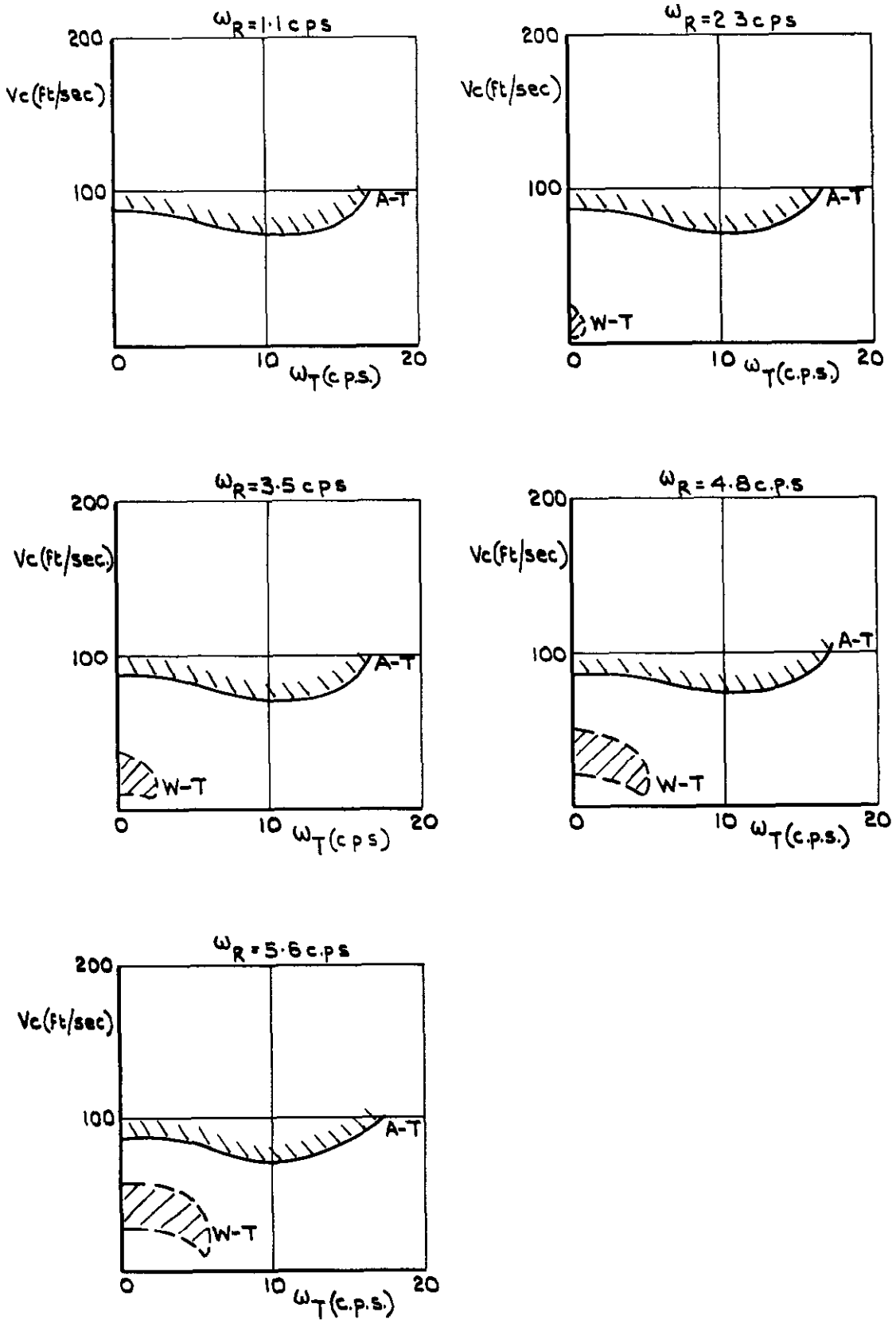

GEARED TAB

FIG. 13. THE VARIATION OF FLUTTER SPEED WITH TAB FREQUENCY FOR SEVERAL VALUES OF WING ROLLING FREQUENCY & WITH No. 4A AILERON CONNECTING SPRING FITTED.

N = −3

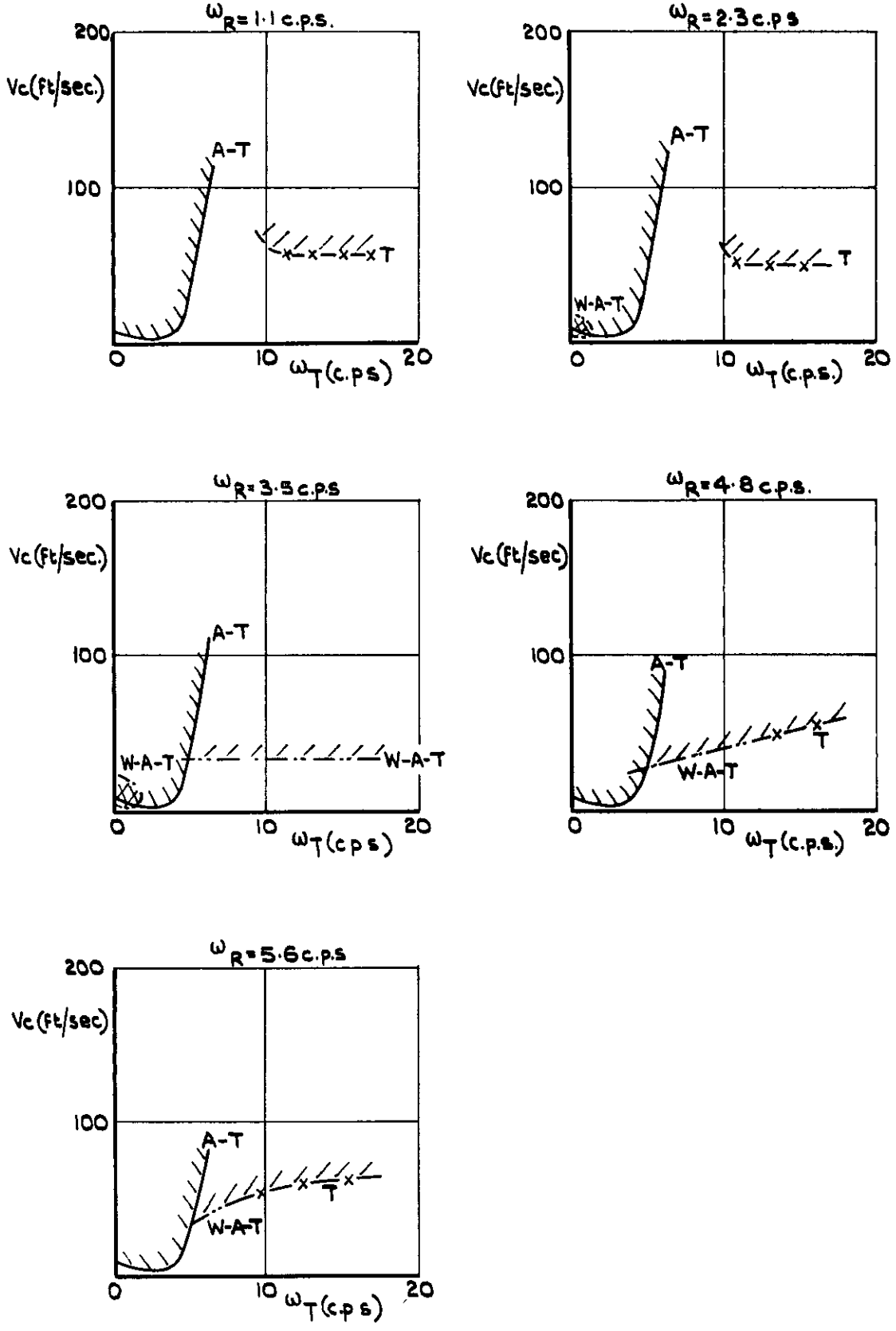

GEARED TAB

FIG. 14. THE VARIATION OF FLUTTER SPEED WITH TAB FREQUENCY FOR SEVERAL VALUES OF WING ROLLING FREQUENCY & WITH No. 1A AILERON CONNECTING SPRING FITTED.

N = −3

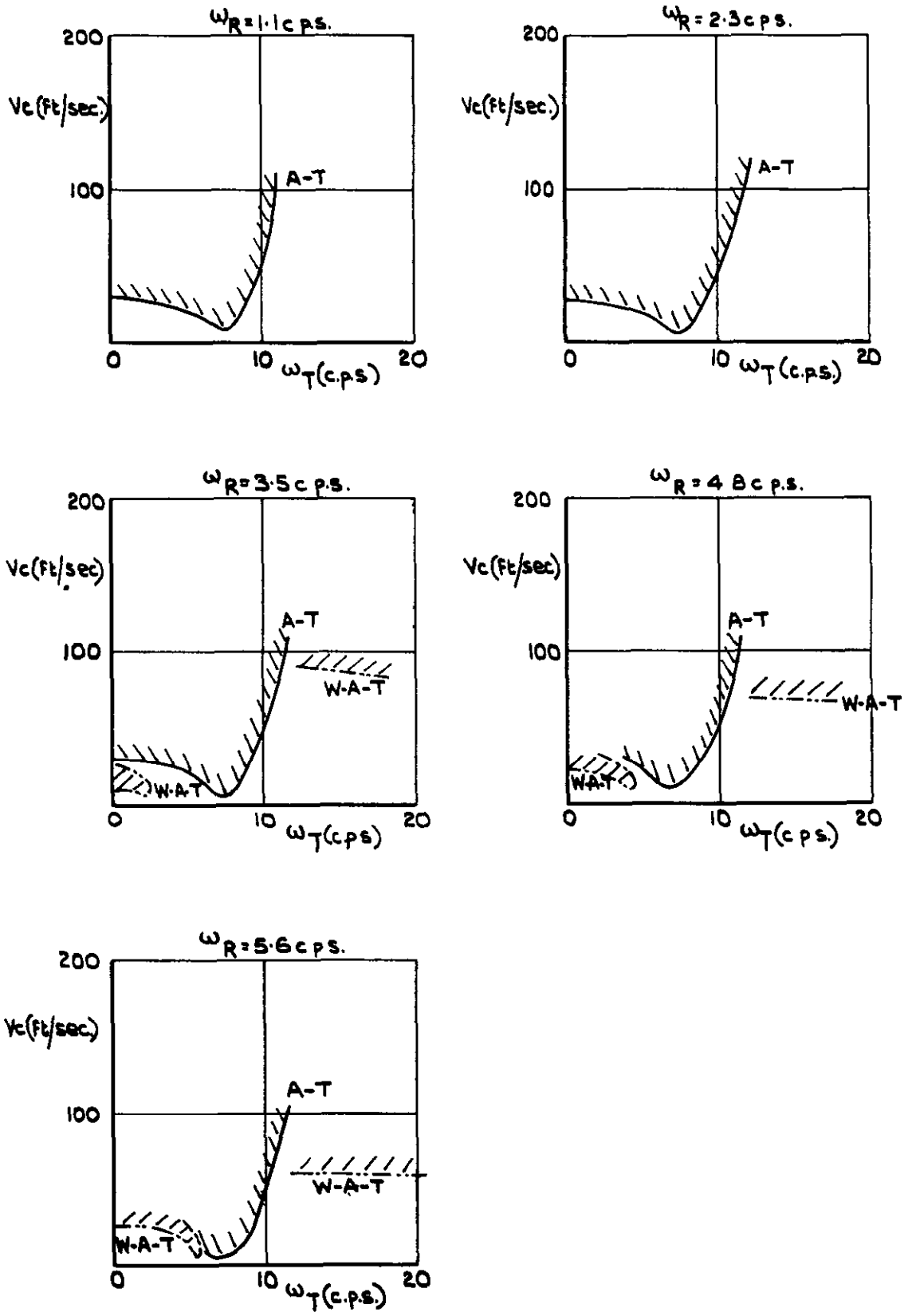

GEARED TAB

FIG. 15. THE VARIATION OF FLUTTER SPEED WITH TAB FREQUENCY FOR SEVERAL VALUES OF WING ROLLING FREQUENCY & WITH No. 2A AILERON CONNECTING SPRING FITTED.

N = -3

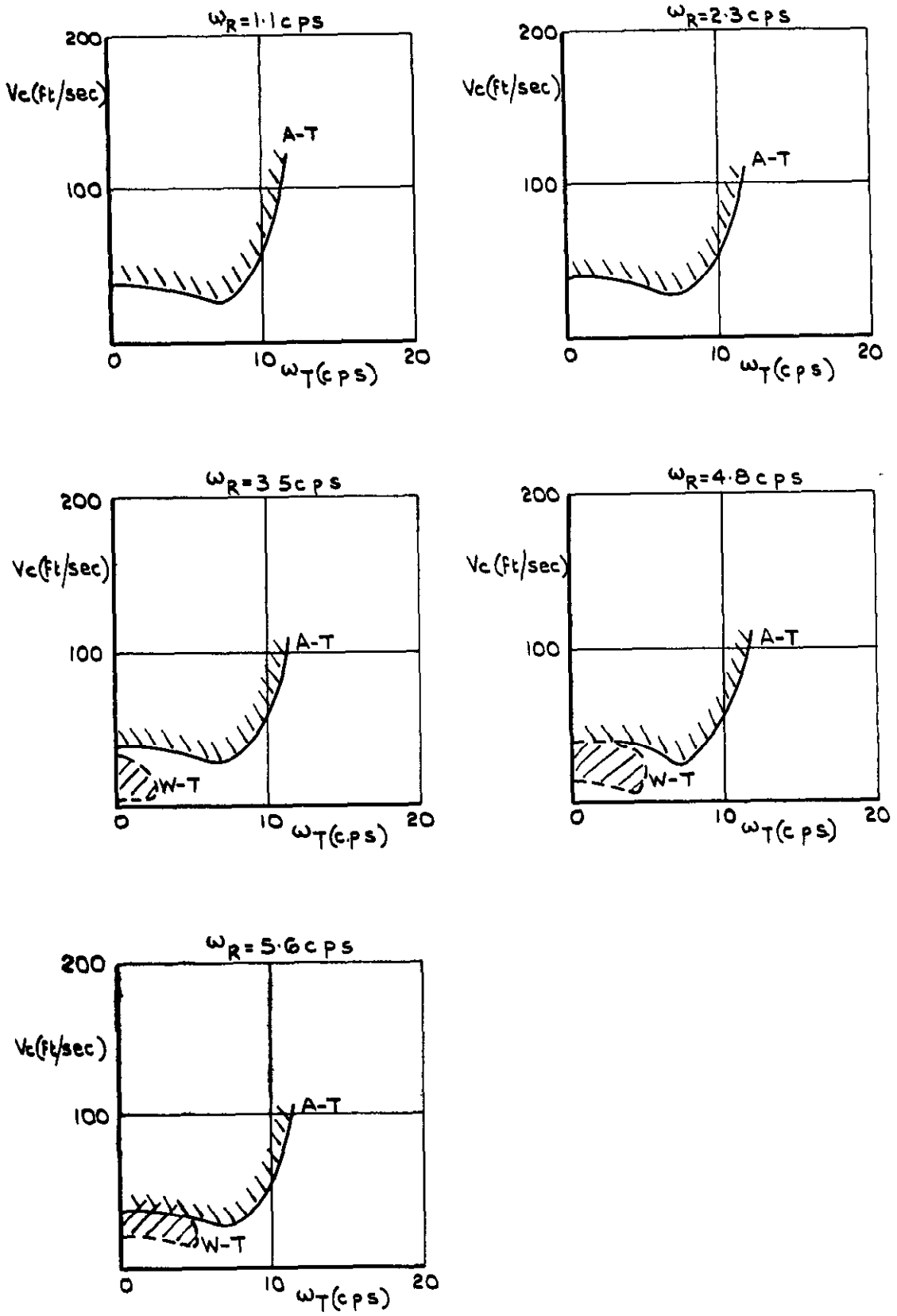

GEARED TAB

FIG.16. THE VARIATION OF FLUTTER SPEED WITH TAB FREQUENCY FOR SEVERAL VALUES OF WING ROLLING FREQUENCY & WITH No. 3A AILERON CONNECTING SPRING FITTED.

N = −3

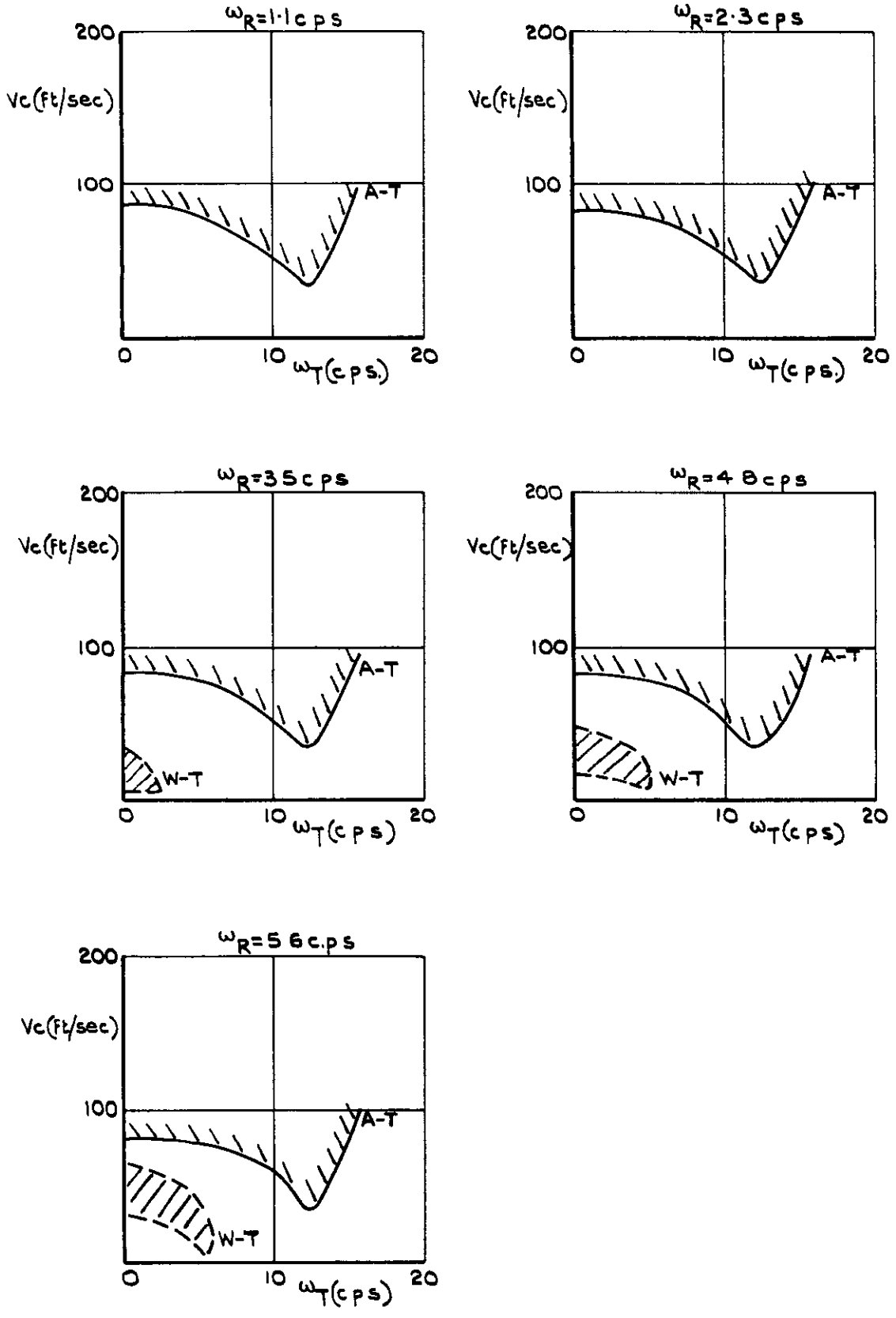

GEARED TAB

FIG. 17. THE VARIATION OF FLUTTER SPEED WITH TAB FREQUENCY FOR SEVERAL VALUES OF WING ROLLING FREQUENCY & WITH No. 4A AILERON CONNECTING SPRING FITTED.

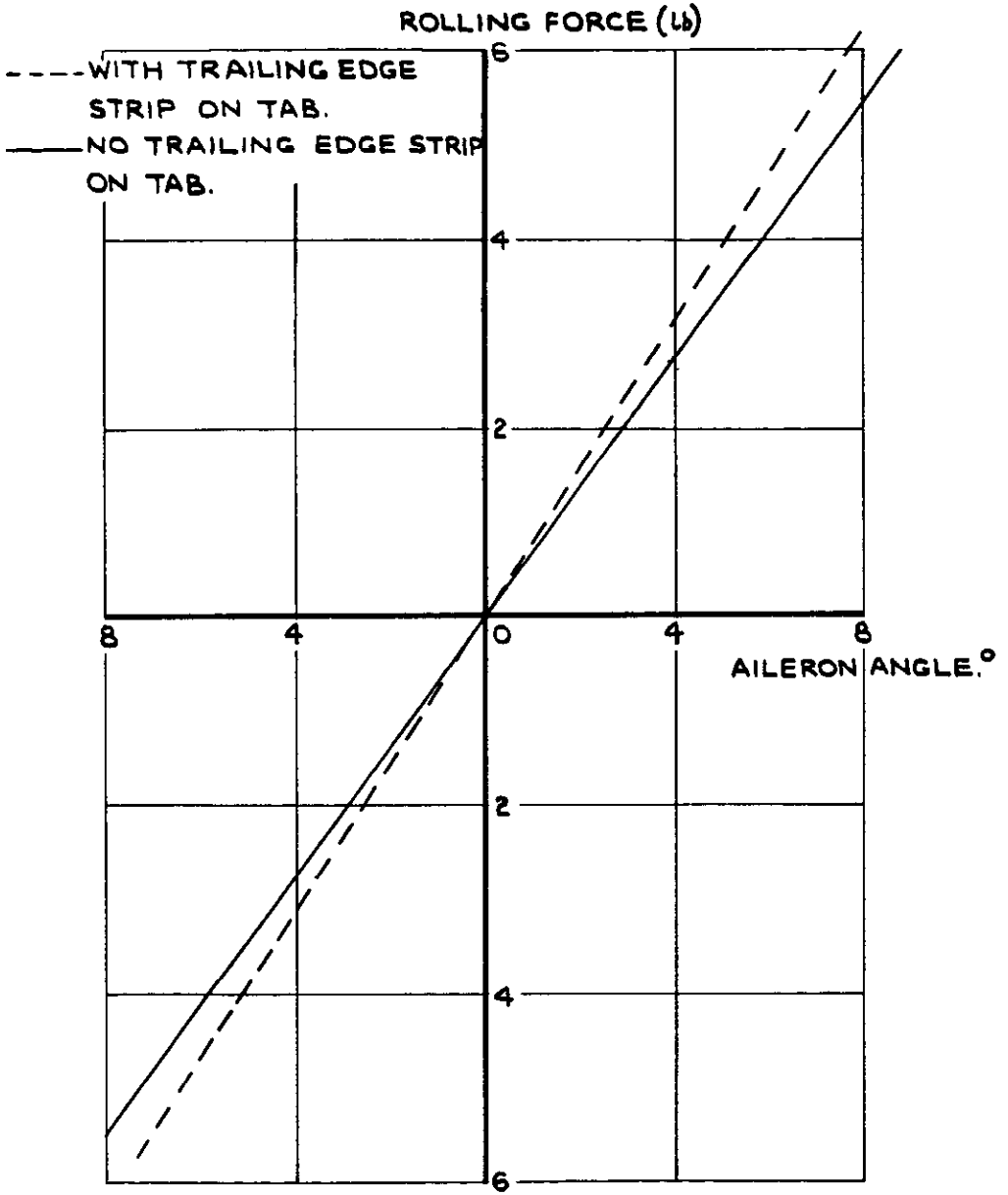

FIG. 18. THE VARIATION OF ROLLING FORCE WITH AILERON ANGLE AT A SPEED OF 100 FT/SEC.

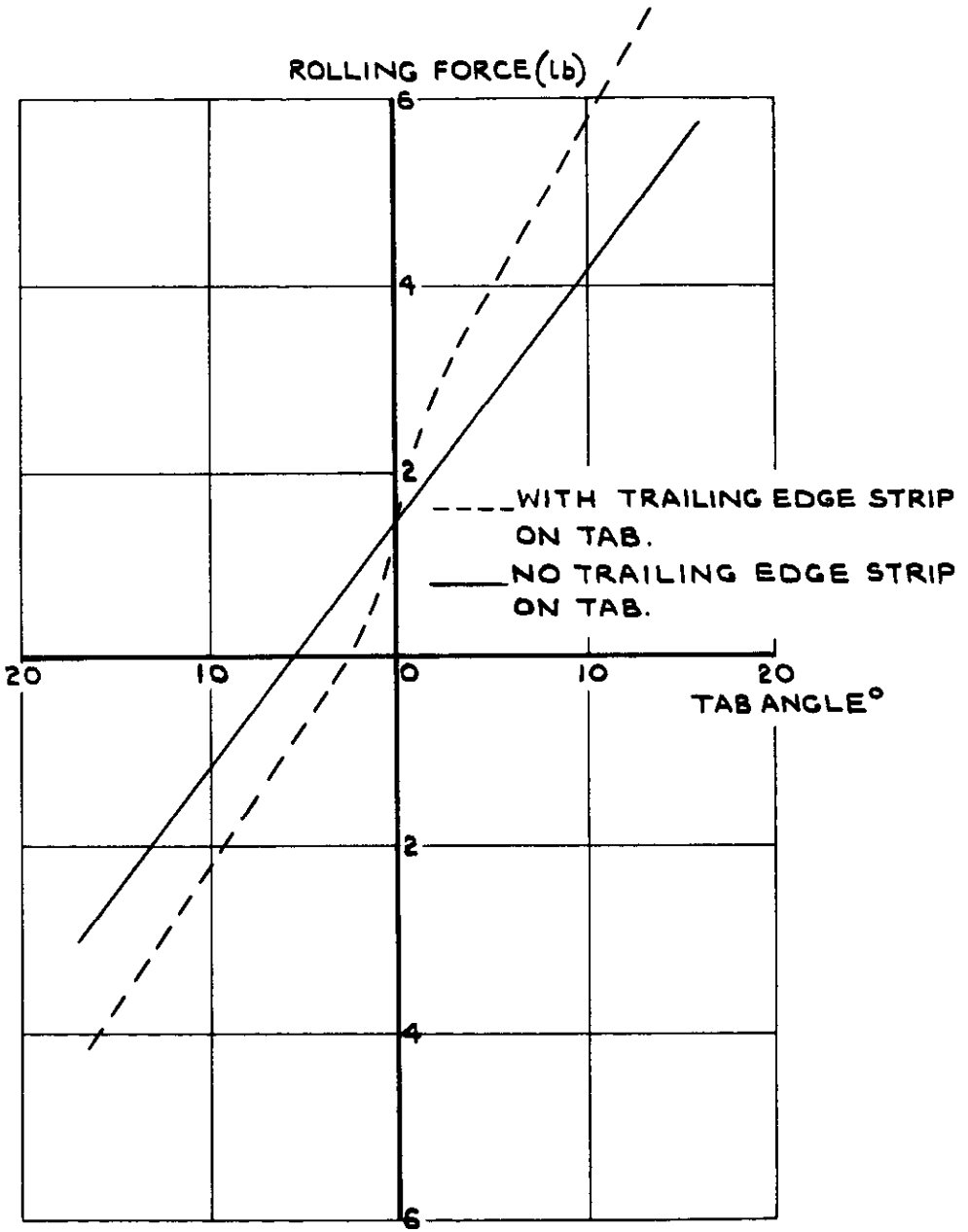

FIG. 19. THE VARIATION OF ROLLING FORCE WITH TAB ANGLE AT A SPEED OF 140 FT/SEC.

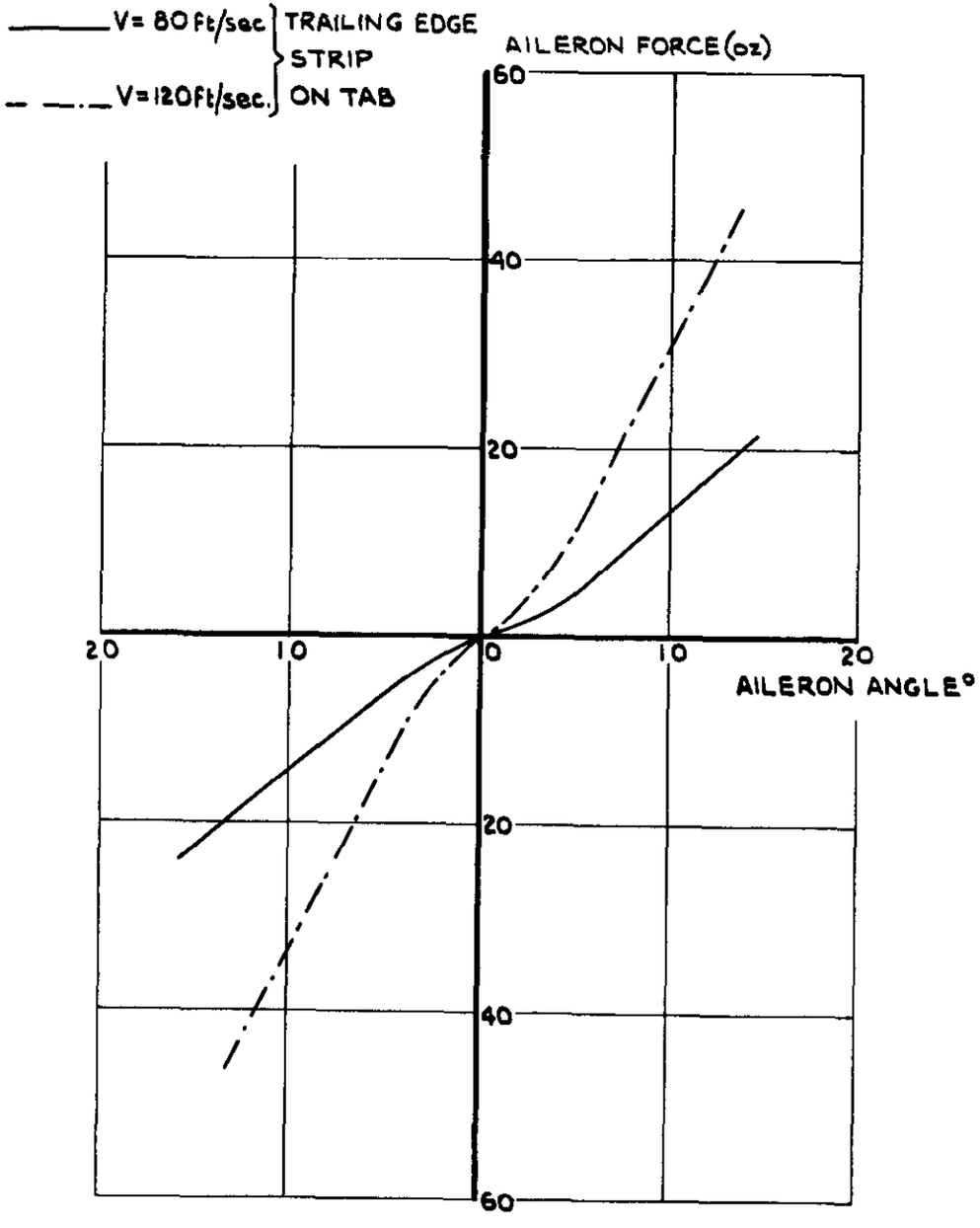

FIG. 20. THE VARIATION OF AILERON DISTURBING FORCE WITH AILERON ANGLE.

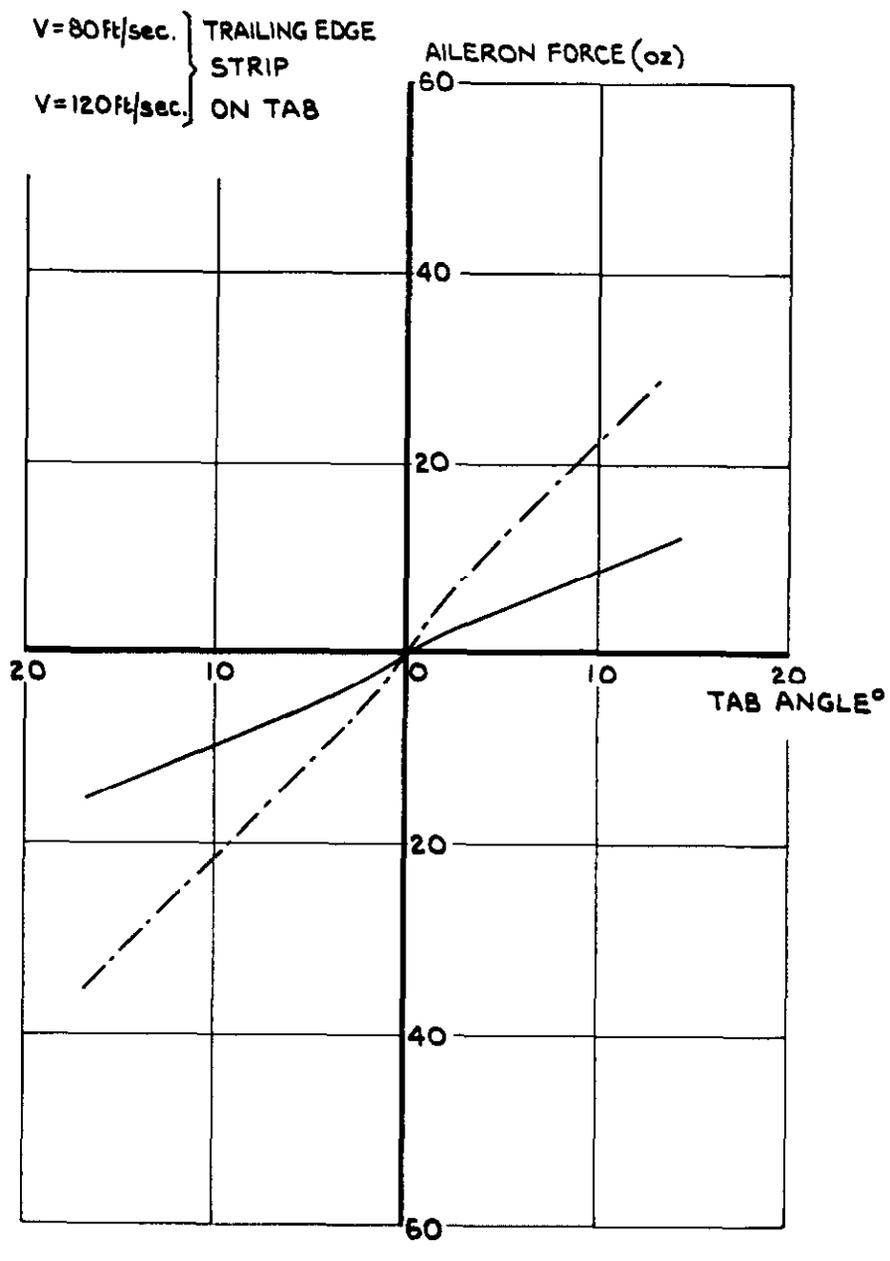

FIG. 21. THE VARIATION OF AILERON RESTORING FORCE WITH TAB ANGLE.

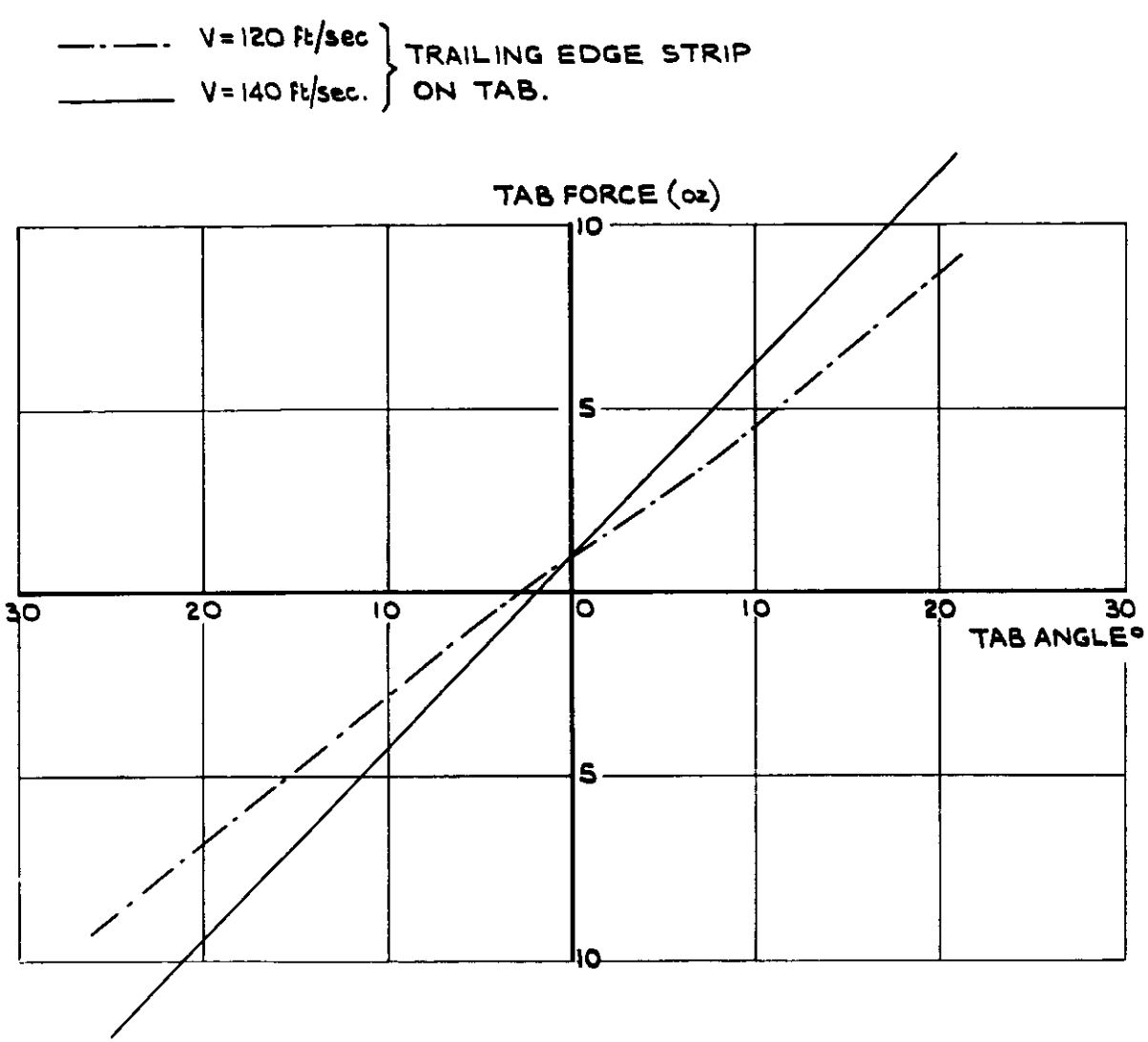

FIG 22. THE VARIATION OF TAB DISTURBING FORCE WITH TAB ANGLE.

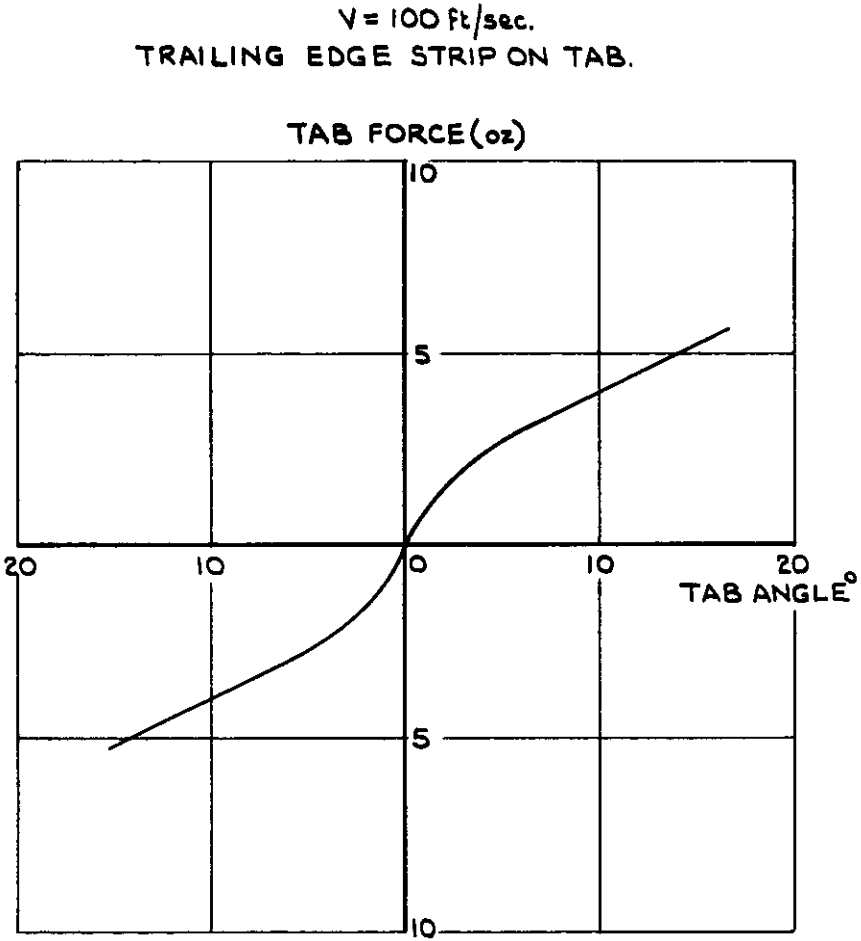

FIG. 23. THE VARIATION OF TAB DISTURBING FORCE WITH TAB ANGLE. (VARIABLE WIND SPEED TESTS)

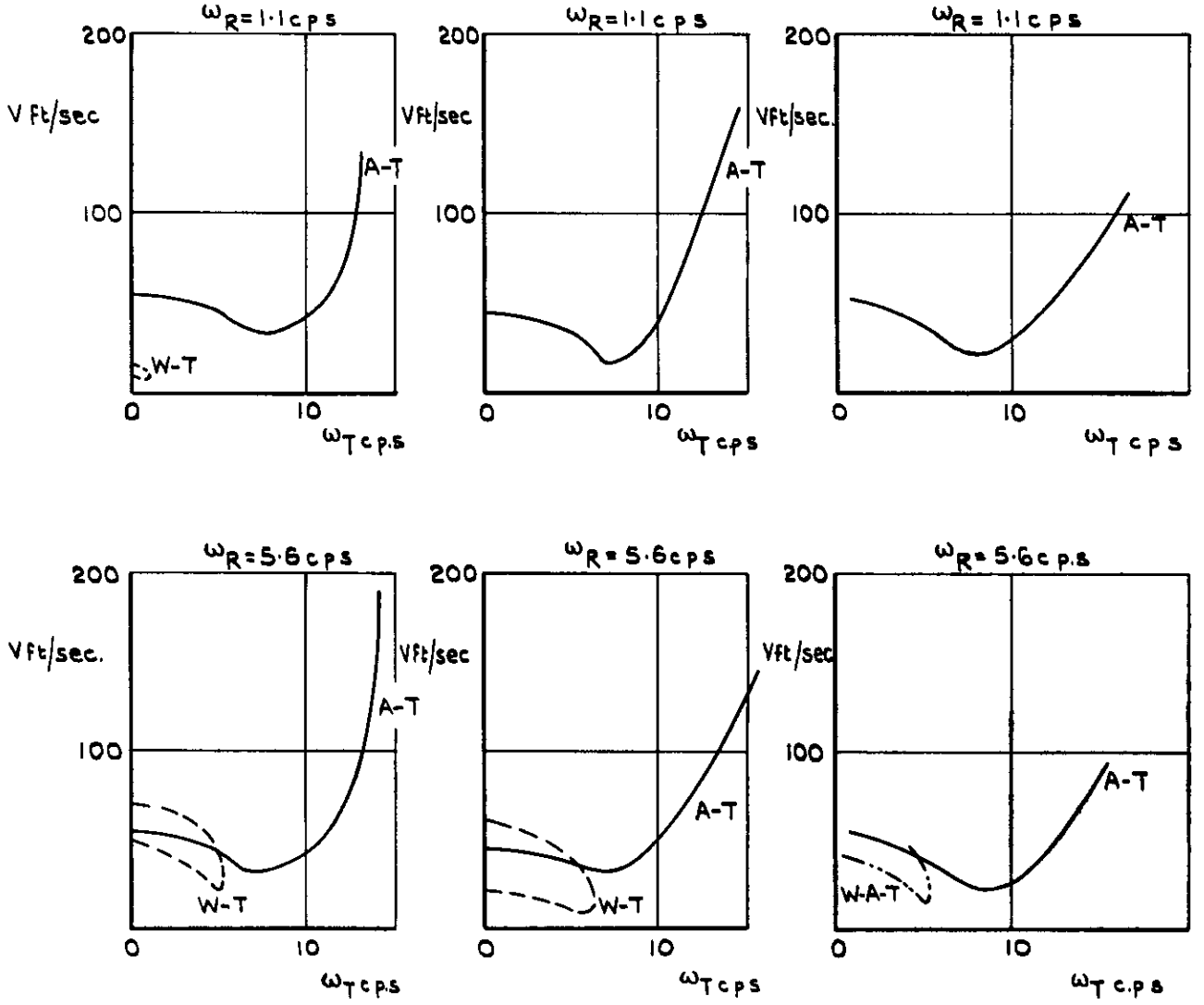

FIG 24. THE CALCULATED VARIATION OF FLUTTER SPEED WITH TAB FREQUENCY COMPARED WITH THE MEASURED VARIATION · FOR TWO VALUES OF WING ROLLING FREQUENCY AND A CONSTANT AILERON FREQUENCY OF 8·8 C.P.S.

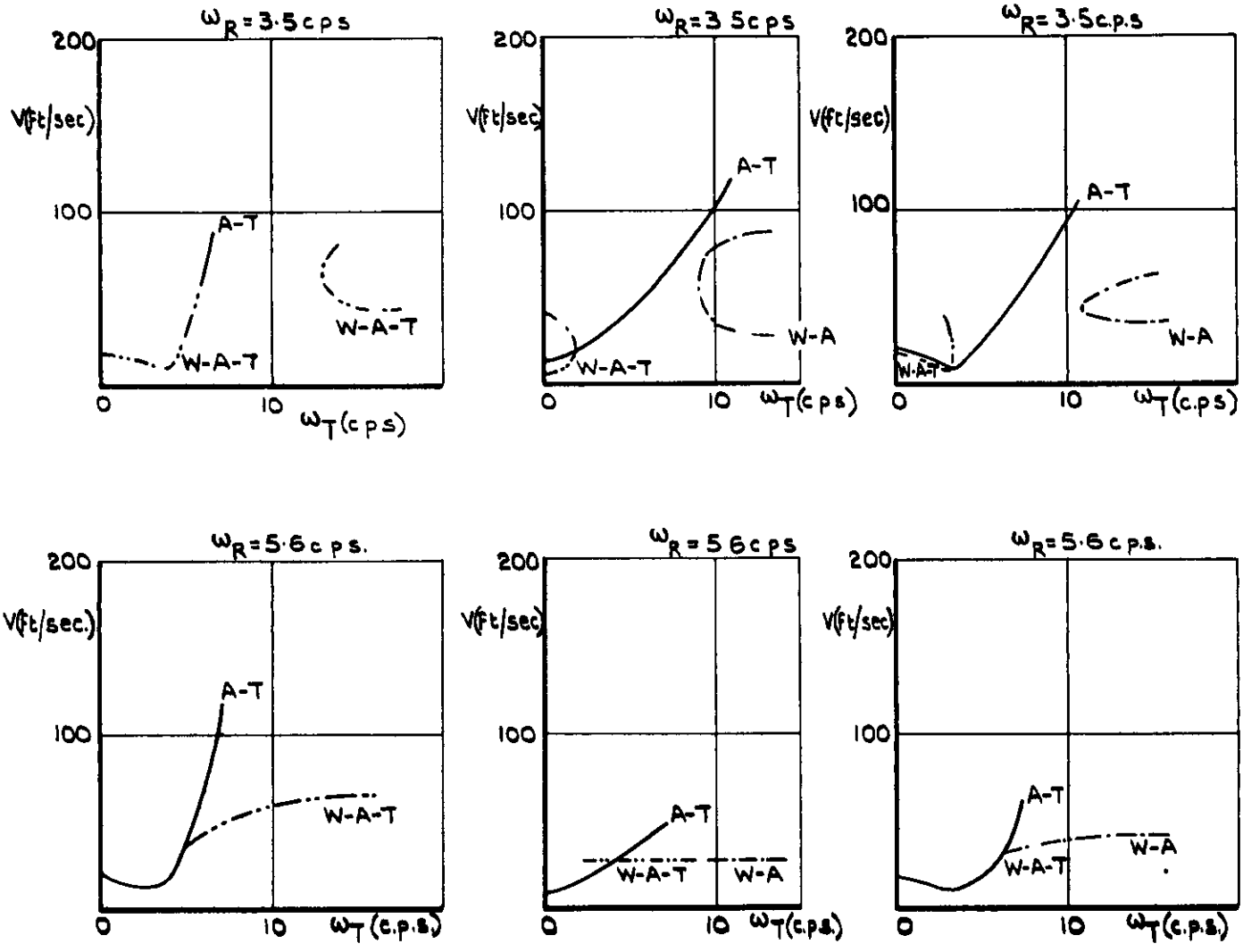

BASED ON STEADY MOTION AERODYNAMIC DERIVATIVES MEASURED ON THIS WING METHOD II

EXPERIMENTAL RESULTS

BASED ON THEORETICAL STEADY MOTION AERODYNAMIC DERIVATIVES METHOD IV

FIG. 25. THE CALCULATED VARIATION OF FLUTTER SPEED WITH TAB FREQUENCY COMPARED WITH THE MEASURED VARIATION FOR TWO VALUES OF WING ROLLING FREQUENCY AND A CONSTANT AILERON FREQUENCY OF 3·6 C.P.S.

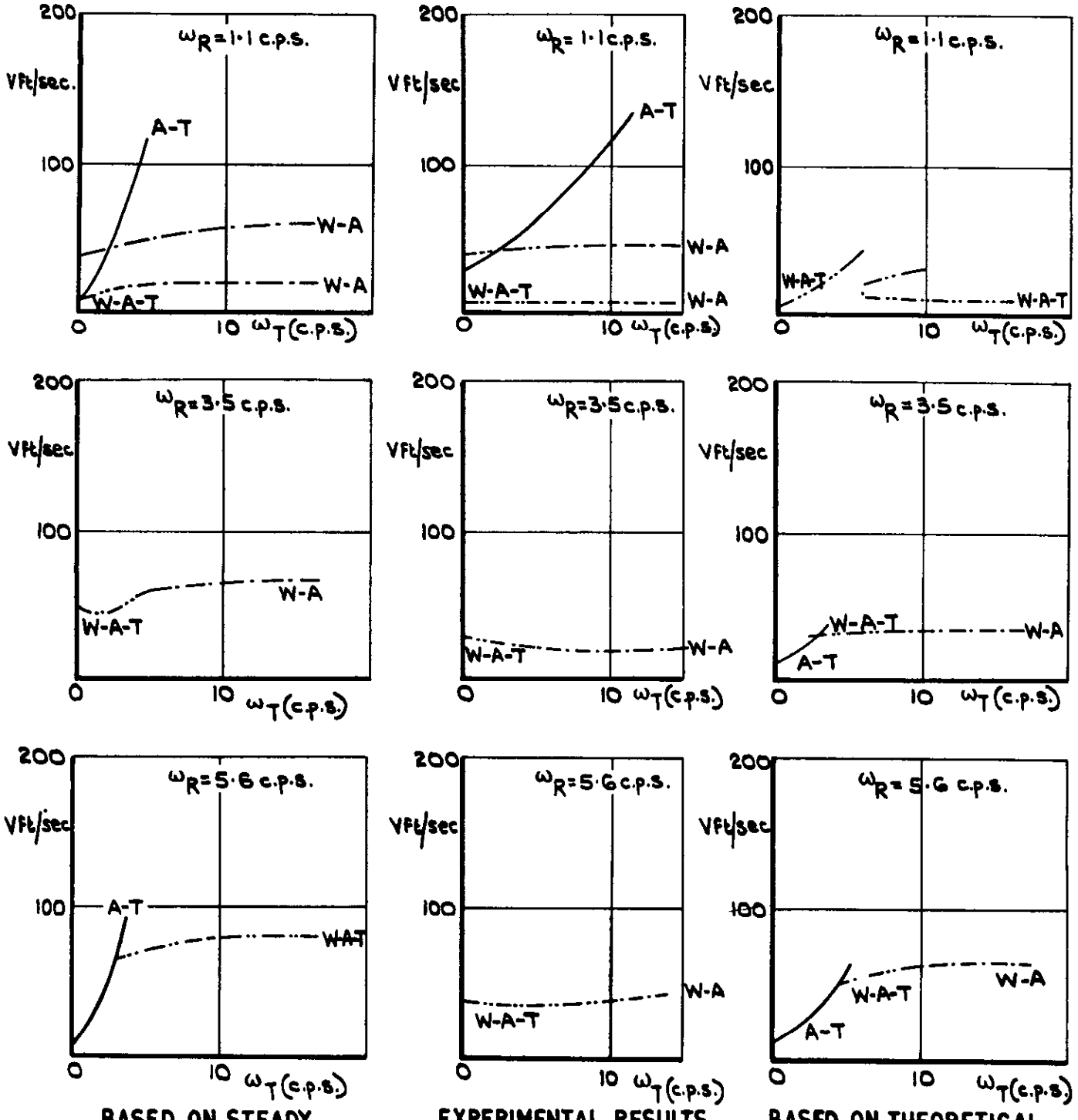

BASED ON STEADY MOTION AERODYNAMIC DERIVATIVES MEASURED ON THIS WING.
METHOD II

EXPERIMENTAL RESULTS.

BASED ON THEORETICAL STEADY MOTION AERODYNAMIC DERIVATIVES.
METHOD IV

FIG. 26. THE CALCULATED VARIATION OF FLUTTER SPEED WITH TAB FREQUENCY COMPARED WITH THE MEASURED VARIATION FOR THREE VALUES OF WING ROLLING FREQUENCY AND FOR A FREE AILERON

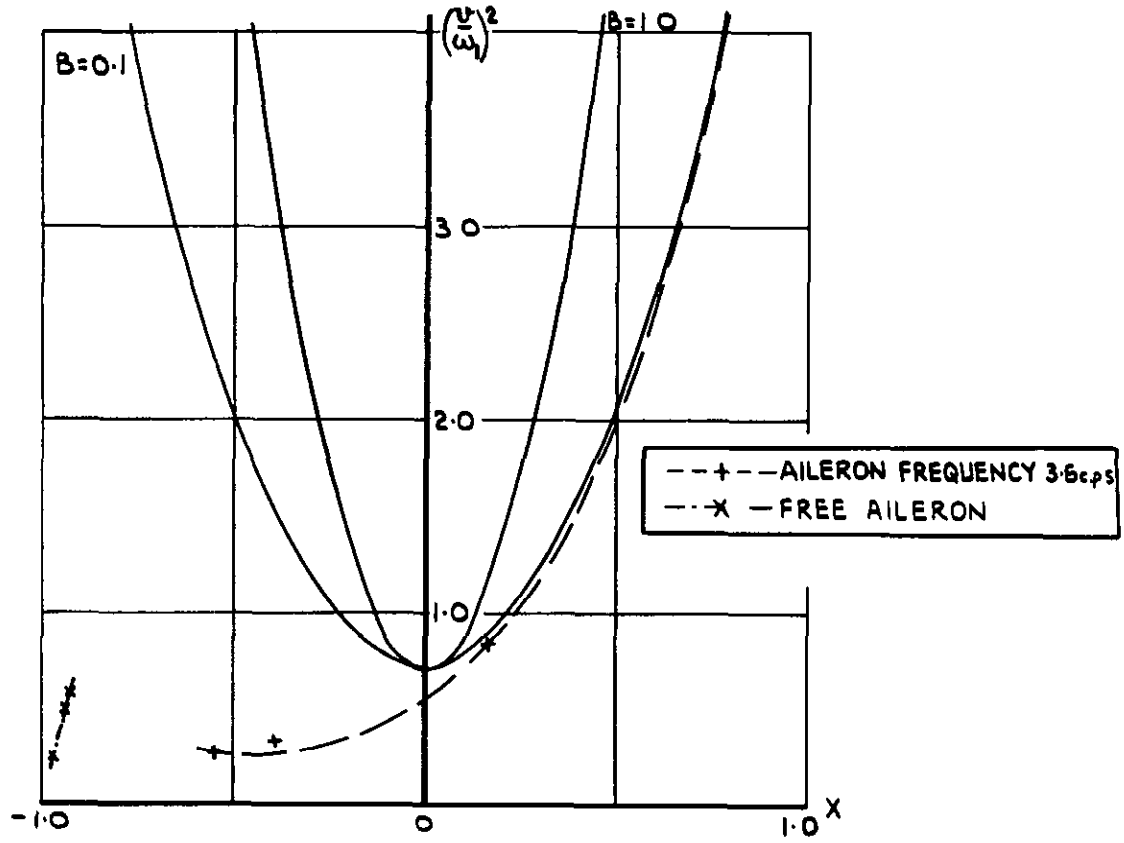

METHOD II DERIVATIVES.

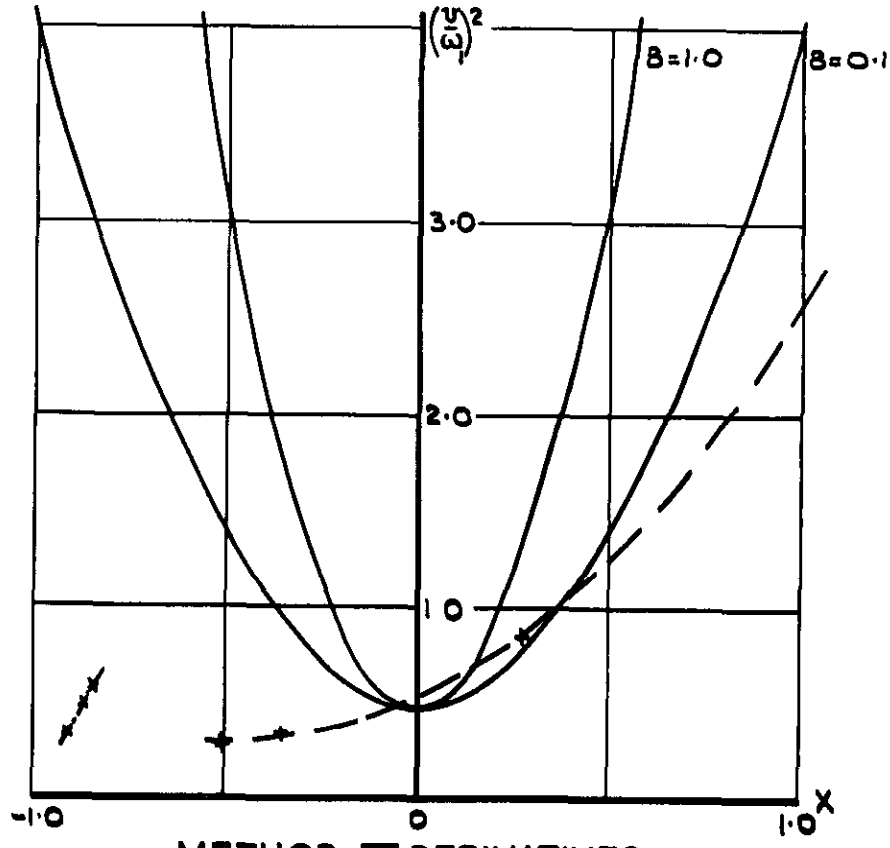

METHOD IV DERIVATIVES

FIG. 27. THE CRITERION BOUNDS OBTAINED FOR WING ROLL – AILERON ROTATION FLUTTER COMPARED WITH THE EXPERIMENTALLY OBTAINED BOUNDS (N=0)

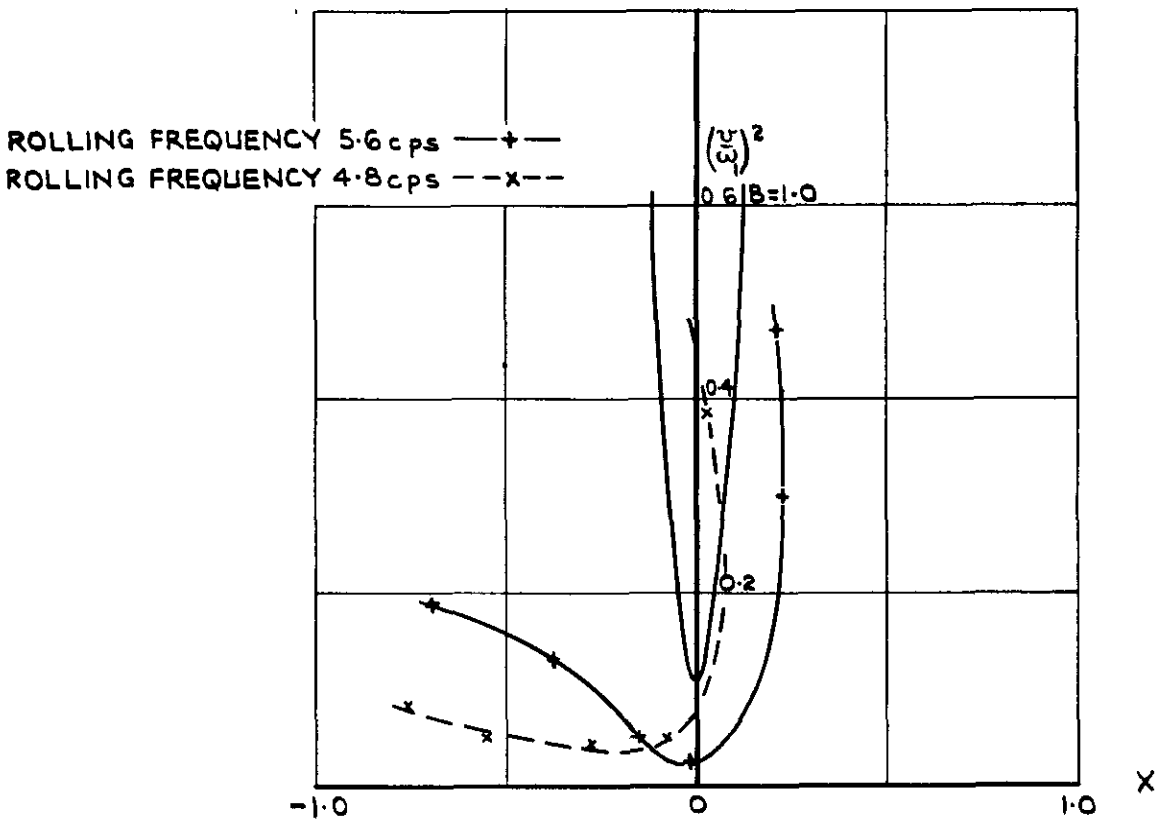

METHOD II DERIVATIVES

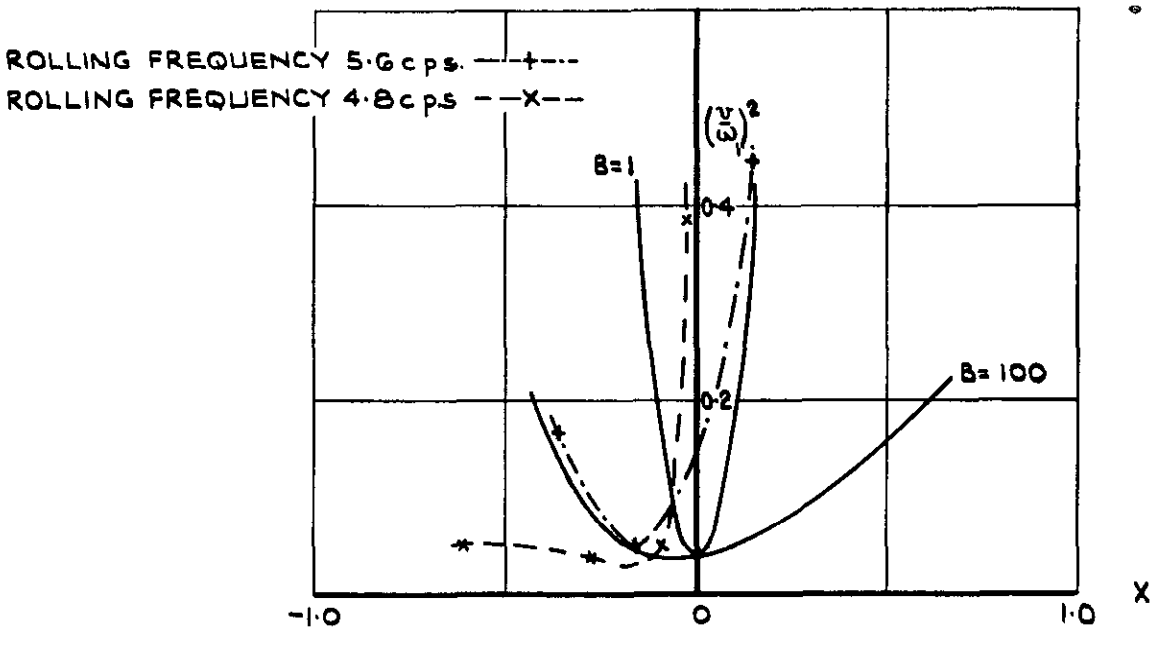

METHOD IV DERIVATIVES

FIG. 28. THE CRITERION BOUNDS FOR WING ROLL-TAB ROTATION FLUTTER COMPARED WITH THE EXPERIMENTALLY OBTAINED BOUNDS (N=0)

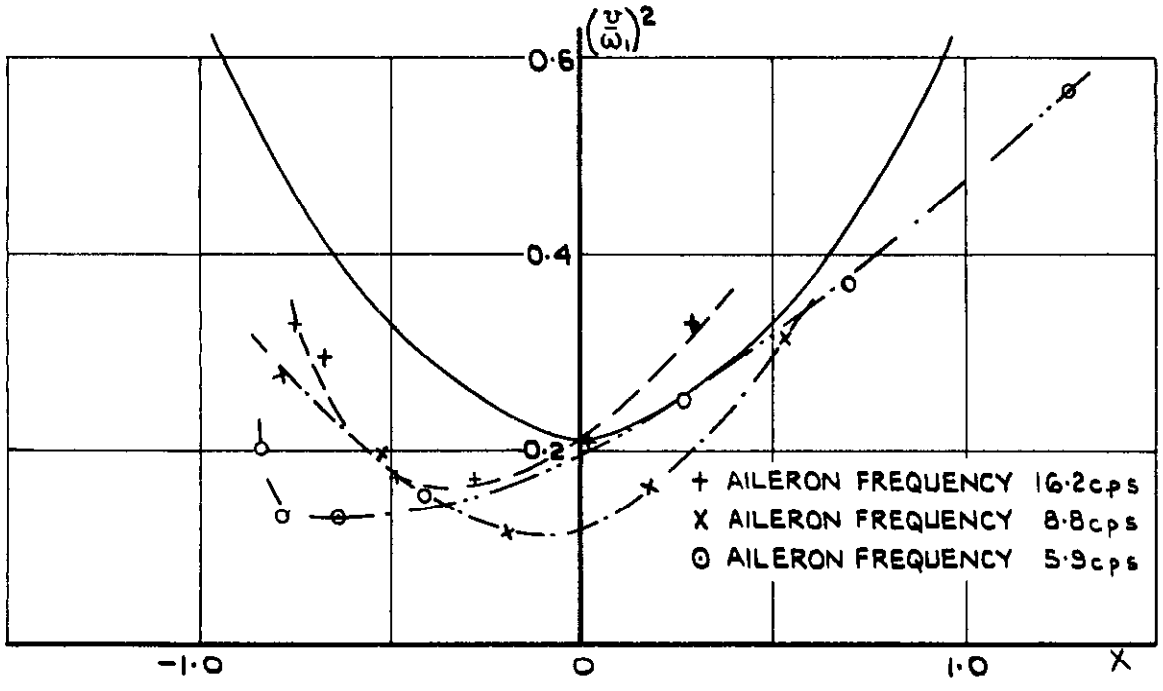

METHOD II DERIVATIVES.

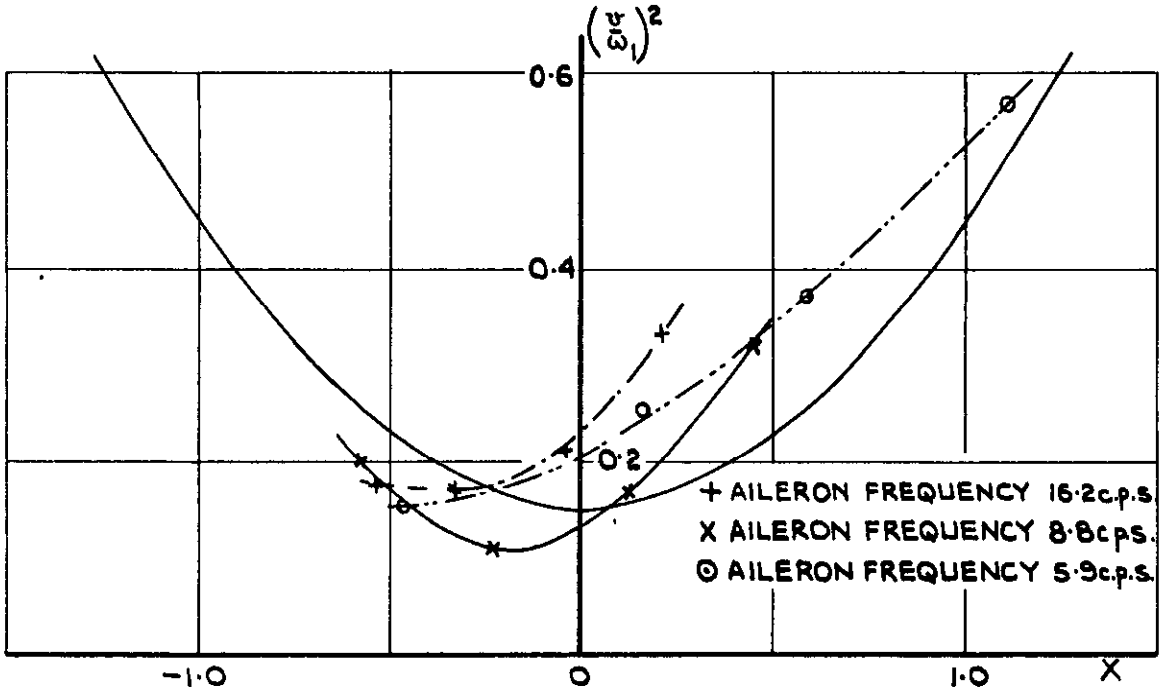

METHOD IV DERIVATIVES.

FIG. 29. THE CRITERION BOUNDS FOR AILERON ROTATION-TAB ROTATION FLUTTER COMPARED WITH THE EXPERIMENTALLY OBTAINED BOUNDS.(N=O)

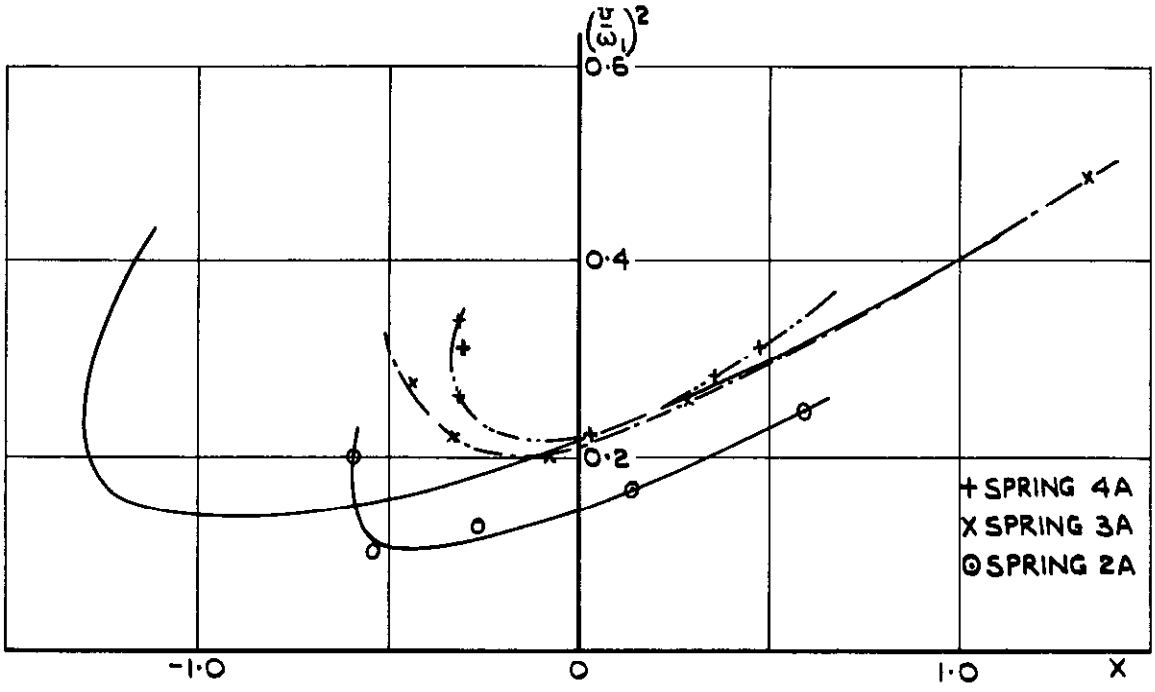

METHOD II DERIVATIVES

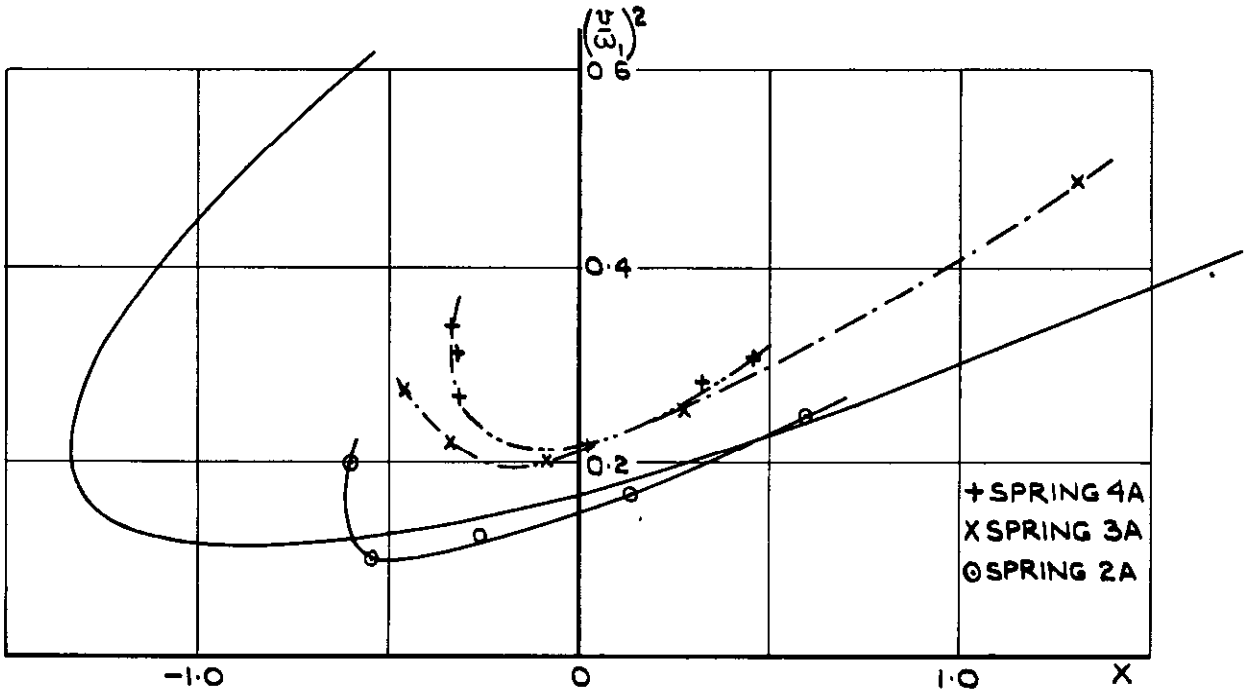

METHOD IV DERIVATIVES

FIG. 30. THE CRITERION BOUNDS FOR AILERON ROTATION-TAB ROTATION FLUTTER COMPARED WITH THE EXPERIMENTALLY OBTAINED BOUNDS (N=+3)

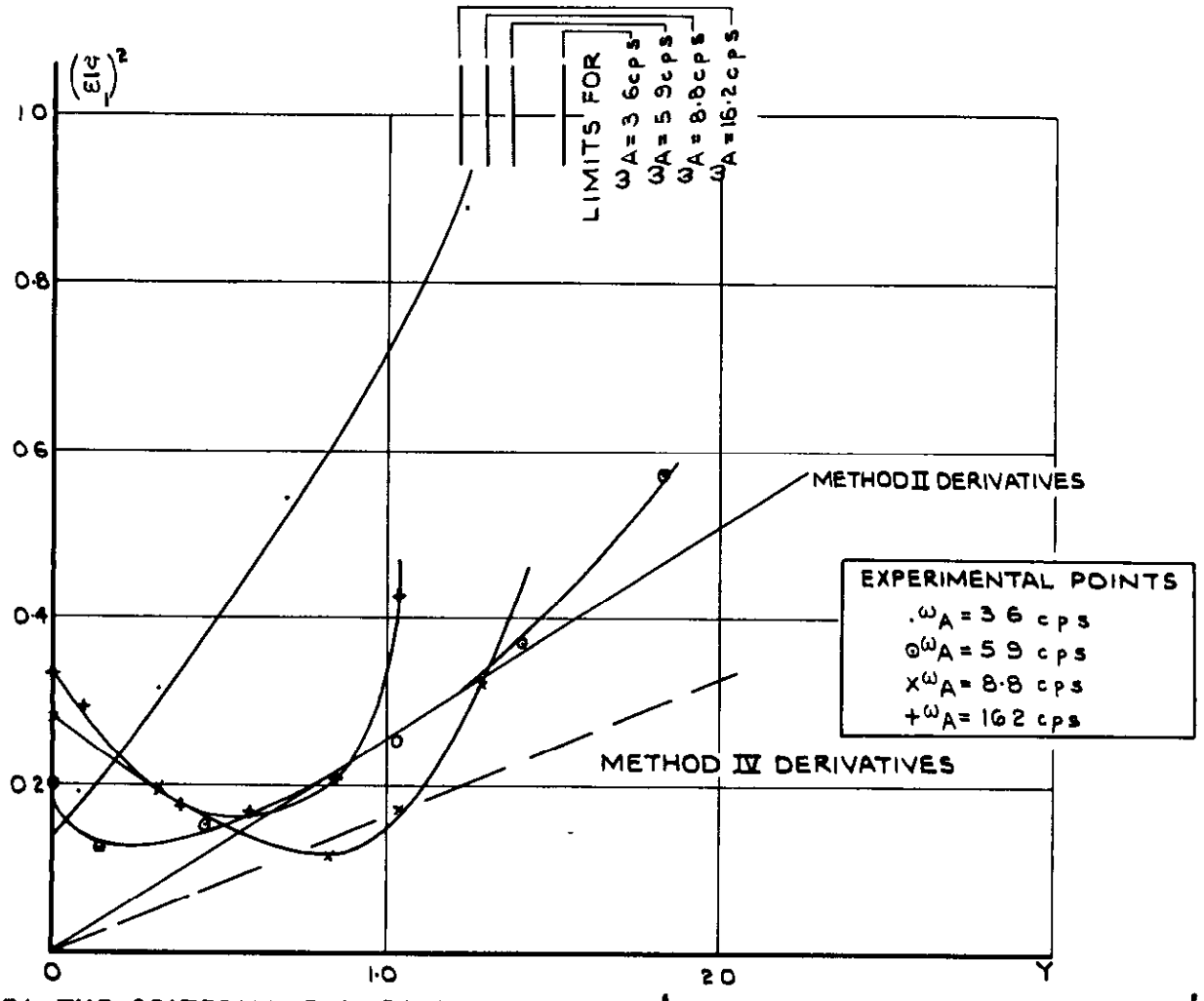

FIG. 31. THE CRITERION BOUNDS BASED ON THE 'SINGLE FREQUENCY APPROXIMATION' FOR AILERON ROTATION - TAB ROTATION FLUTTER (N = 0) COMPARED WITH THE EXPERIMENTALLY OBTAINED BOUNDS

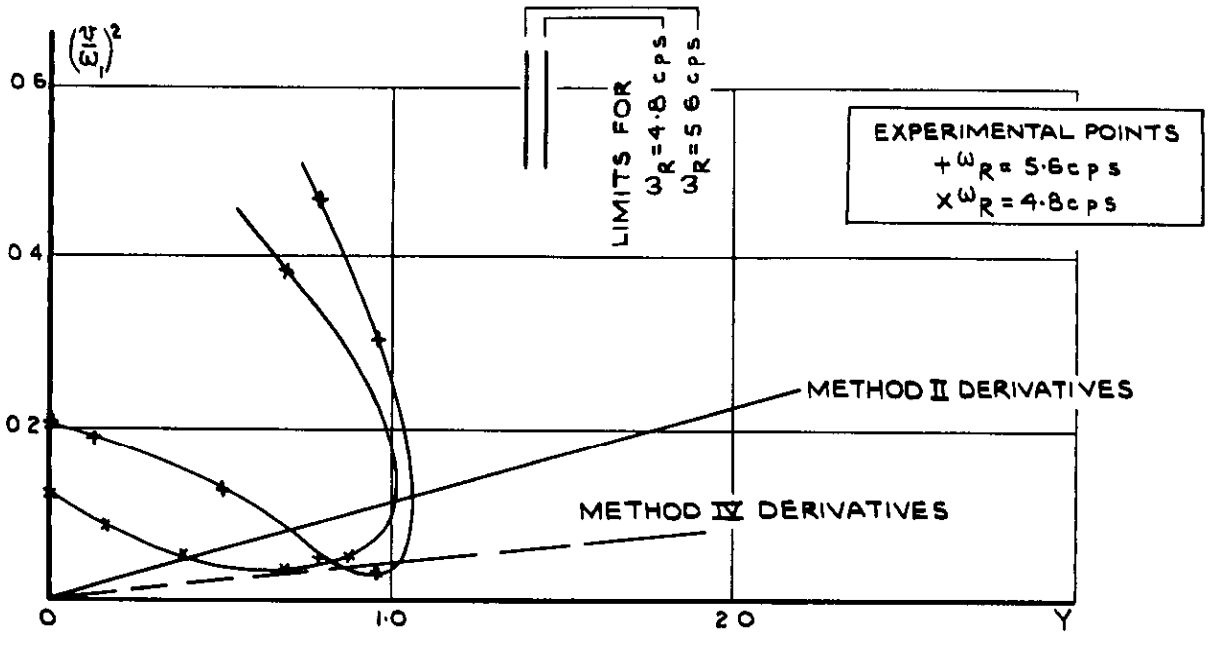

FIG. 32. THE CRITERION BOUNDS BASED ON THE 'SINGLE FREQUENCY APPROXIMATION' FOR WING ROLL - TAB ROTATION FLUTTER (N = 0) COMPARED WITH THE EXPERIMENTALLY OBTAINED BOUNDS

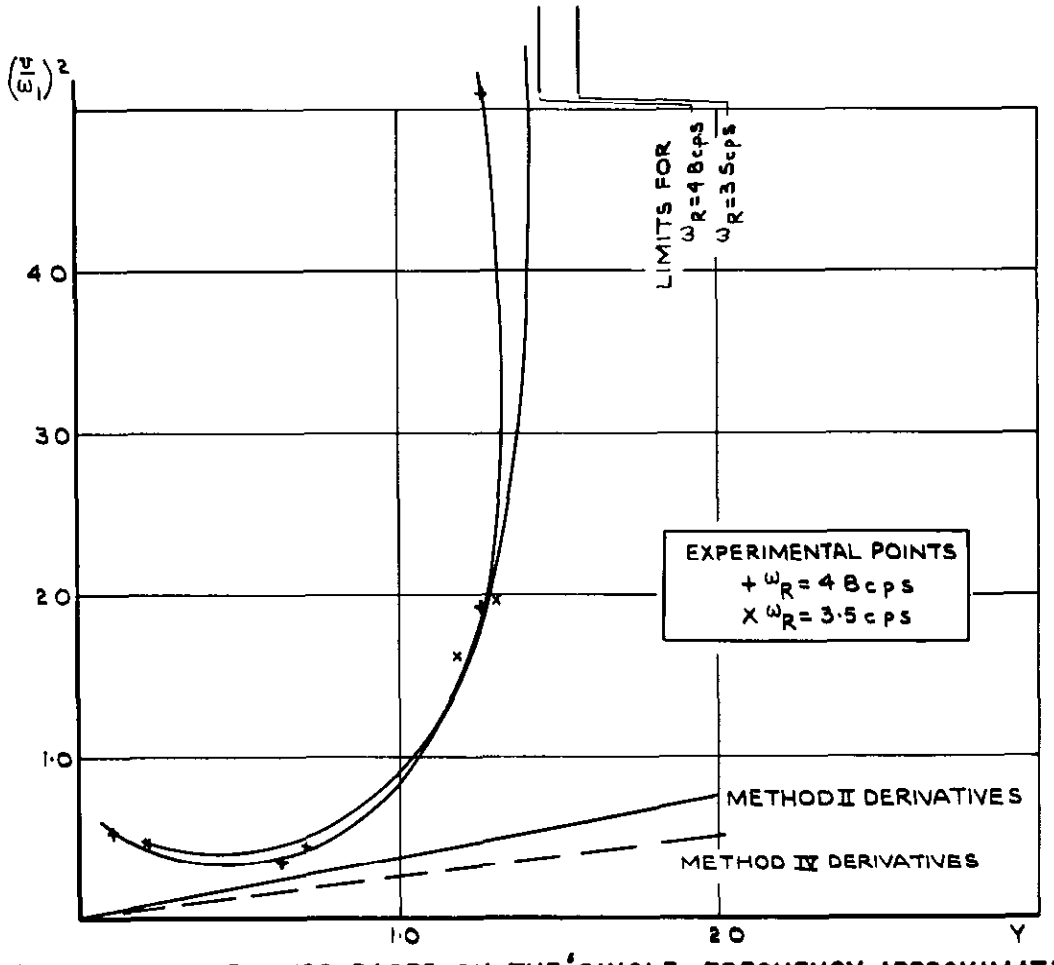

FIG. 33. THE CRITERION BOUNDS BASED ON THE 'SINGLE FREQUENCY APPROXIMATION' FOR WING ROLL-AILERON ROTATION FLUTTER (N = - 3) COMPARED WITH EXPERIMENTALLY OBTAINED BOUNDS

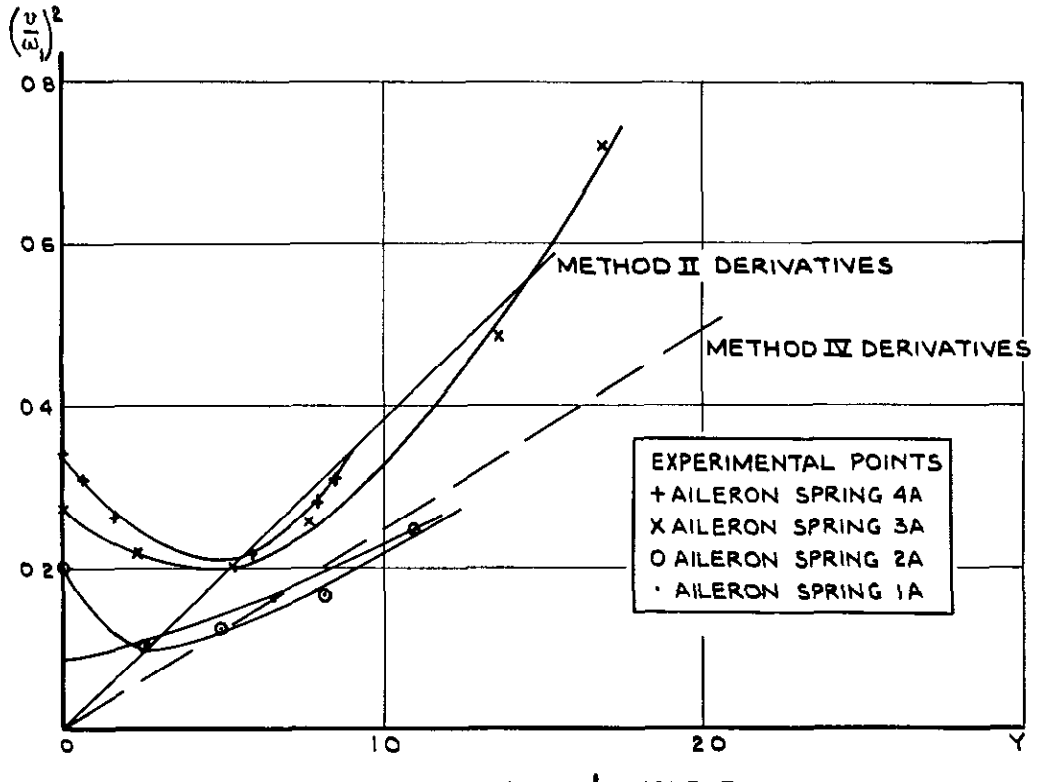

FIG 34 THE CRITERION BOUNDS BASED ON THE 'SINGLE FREQUENCY APPROXIMATION' FOR AILERON ROTATION-TAB ROTATION FLUTTER (N = + 3) COMPARED WITH THE EXPERIMENTALLY OBTAINED BOUNDS

A R C C P No. 715

533.6.013.422 :
533.693 :
533.694.512 :
533.694.58

A COMPARISON OF THE MEASURED AND PREDICTED FLUTTER CHARACTERISTICS OF A WING-AILERON-TAB MODEL.
Hall, H. August 1963.

The paper presents results of wind tunnel flutter tests using a wing-aileron-tab model on which it was possible to represent any of the following tab systems; spring, geared, trim or servo. Prediction of the flutter characteristics has been made in the trim tab case using three sets of aerodynamic derivatives and fair agreement has been reached with the measured characteristics. A comparison has also been made of the measured characteristics with those predicted by the latest flutter criteria and possible modifications to the basic flutter frequency

(Over)

A R.C. C P. No. 715

533.6.013.422 :
533.693 :
533.694.512 :
533.694.58

A COMPARISON OF THE MEASURED AND PREDICTED FLUTTER CHARACTERISTICS OF A WING-AILERON-TAB MODEL.
Hall, H. August 1963.

The paper presents results of wind tunnel flutter tests using a wing-aileron-tab model on which it was possible to represent any of the following tab systems; spring, geared, trim or servo. Prediction of the flutter characteristics has been made in the trim tab case using three sets of aerodynamic derivatives and fair agreement has been reached with the measured characteristics. A comparison has also been made of the measured characteristics with those predicted by the latest flutter criteria and possible modifications to the basic flutter frequency

(Over)

A R.C C.P. No. 715

533.6.013.422 :
533.693 :
533.694.512 :
533.694.58

A COMPARISON OF THE MEASURED AND PREDICTED FLUTTER CHARACTERISTICS OF A WING-AILERON-TAB MODEL.
Hall, H. August 1963.

The paper presents results of wind tunnel flutter tests using a wing-aileron-tab model on which it was possible to represent any of the following tab systems; spring, geared, trim or servo. Prediction of the flutter characteristics has been made in the trim tab case using three sets of aerodynamic derivatives and fair agreement has been reached with the measured characteristics. A comparison has also been made of the measured characteristics with those predicted by the latest flutter criteria and possible modifications to the basic flutter frequency

(Over)

assumption used in deriving the criteria are discussed. One modification suggested is such that the basic flutter frequency is virtually dependent on the frequency in a single degree of freedom. The criterion form that results from such a single frequency approximation is investigated.

assumption used in deriving the criteria are discussed. One modification suggested is such that the basic flutter frequency is virtually dependent on the frequency in a single degree of freedom. The criterion form that results from such a single frequency approximation is investigated.

assumption used in deriving the criteria are discussed. One modification suggested is such that the basic flutter frequency is virtually dependant on the frequency in a single degree of freedom. The criterion form that results from such a single frequency approximation is investigated.

Published by
HER MAJESTY'S STATIONERY OFFICE
To be purchased from
York House, Kingsway, London, W C 2
423 Oxford Street, London, W 1
13A Castle Street, Edinburgh 2
109 St Mary Street, Cardiff
39 King Street, Manchester 2
50 Fairfax Street, Bristol 1
35 Smallbrook, Ringway, Birmingham 5
80 Chichester Street, Belfast 1
or through any bookseller

S O Code No 23-9015-15